Broadband Search for Axion Dark Matter via Shift Current

Dan Kondo,[1,*] Takahiro Morimoto,[2,†] Genta Osaki,[3,‡] and Thanaporn Sichanugrist[3,§]

[1]*Kavli Institute for the Physics and Mathematics of the Universe (WPI), University of Tokyo Institutes for Advanced Study, University of Tokyo, Kashiwa 277-8583, Japan*
[2]*Department of Applied Physics, The University of Tokyo, Tokyo 113-8656, Japan*
[3]*Department of Physics, The University of Tokyo, Tokyo 113-8656, Japan*

(Dated: May 23, 2025)

We propose a novel method to detect axion dark matter based on a topological phenomenon known as the shift current. We exploit the second-order nonlinearity of the shift current by applying a strong oscillating electric field. This field enhances the axion-induced shift current signal and downconverts its frequency to a more accessible range. The non-dissipative nature of the shift current allows us to achieve broadband detection via difference frequency generation. We demonstrate, using Type-I Weyl semimetal TaAs property, the possibility of probing the parameter space of the QCD axion in the mass range of $\mathcal{O}(10)$ - $\mathcal{O}(100)$ meV corresponding to the photon coupling of $g_{a\gamma\gamma} \simeq \mathcal{O}(10^{-12})$ - $\mathcal{O}(10^{-11})$ GeV^{-1}, respectively.

I. INTRODUCTION

The identification of dark matter is a long-standing problem in particle physics, cosmology, and astrophysics. Its particle-physics properties, such as its mass and the coupling to the standard model particles, are largely unknown. One of the promising candidates for dark matter is the axion or axion-like particle (ALP). Axion is a Nambu-Goldstone boson arising from global U(1) Peccei-Quinn (PQ) symmetry [1, 2] that solves the strong CP problem [3]. It is expected that axions or ALPs could have a feeble coupling to photons [4–8]. (For comprehensive reviews, see [9–16]). At present, one of the most promising approaches to look for the axion dark matter is to utilize the axion-photon conversion in external electric or magnetic fields [17]. In particular, cavity haloscope experiments utilize the cavity resonance applied with an external strong magnetic field to detect the axion-induced photons [18]. This has great sensitivity mainly at the dark matter mass range $\mathcal{O}(1)$-$\mathcal{O}(100)$ μeV. However, at higher axion masses, the corresponding signal frequencies exceed the typical resonant frequency of the conventional cavity, and such a region is still remains to be probed.

In this Letter, we propose a novel method for broadband detection of axion dark matter of relatively high mass $\mathcal{O}(100)$ meV using a topological phenomenon called "shift current". The shift current is a non-dissipative, nonlinear optical response generated in ferroelectric materials and is a bulk photovoltaic effect (i.e., a light-induced direct current in crystals with an internal structure that lacks inversion symmetry, arising from asymmetric electron motion during optical excitation, and occurring without the need for conventional semiconductor junctions) [19–23]. It has been applied in studies of terahertz (THz) dynamics [24], corresponding to physics with the energy scale of meV and higher.

Our axion dark matter search idea with the shift current is as follows. First, we apply a static magnetic field to convert axions to an electric field. Second, we apply another strong oscillating electric field to enhance the output signal. Since the shift current is a non-linear response, two fields together can interact with a material and induce an enhanced axion shift current to be observed. The frequency of the resulting signal is determined by the frequency difference of the two input fields. Therefore, when the frequency of the axion-induced electric field aligns with or around that of the experimental field, a high-frequency dark matter field can generate a DC or lower-frequency signal, which is more readily detectable. In this way, by changing the frequency of the experimental field to several values, one can search for the axion dark matter signal in a desired mass range. In particular, with one fixed frequency of the experimental field, the simultaneously detectable range is roughly determined by the band structure of the material and the frequency of the experimental field itself. The shift current fundamentally arises from a spatial shift in the quantum wave function of electronic states during state transitions. Due to its quantum nature, the output shift current exhibits high tolerance to defects, while offering a fast temporal response [25]. Importantly, this non-dissipative nature allows us to achieve broadband detection via difference frequency generation with a stable conductivity without suppression from the electron scattering effect.

We summarize the important features of the shift current that we take advantage of as follows:

- Nonlinearity: an enhancement from the experimentally applied electric field, and reduction of a high-frequency dark matter input field to DC or lower frequencies.

- Non-dissipative nature: signal amplitude is insensitive to impurity and a broadband search is allowed.

* dan.kondo@ipmu.jp
† morimoto@ap.t.u-tokyo.ac.jp
‡ osaki@hep-th.phys.s.u-tokyo.ac.jp
§ thanaporn@hep-th.phys.s.u-tokyo.ac.jp

Based on our method, we demonstrate that, using Type-I Weyl semimetal TaAs, it is possible to probe the parameter space of QCD axions in the mass range of $\mathcal{O}(10)$ - $\mathcal{O}(100)$ meV with the output signal frequency reduced to DC or below $\mathcal{O}(1)$ THz.

The structure of this Letter is as follows. We discuss the axion-induced electric field and the idea of our axion search, utilizing the shift current and difference frequency generation with an additional oscillating input experimental electric field. Then, we introduce the material and derive the sensitivity for axion detection. Lastly, we conclude and discuss the result.

II. AXION-INDUCED SHIFT CURRENT

In the presence of axion dark matter under a magnetic field, the axion can induce the electric field through axion-photon coupling given by

$$\mathcal{L} \supset -\frac{g_{a\gamma\gamma}}{4} a F_{\mu\nu}\tilde{F}^{\mu\nu} = g_{a\gamma\gamma} a \boldsymbol{E}\cdot\boldsymbol{B}, \tag{1}$$

where a is the axion field and F is the electro-magnetic field strength, $\tilde{F}^{\mu\nu} = \epsilon^{\mu\nu\rho\sigma}F_{\rho\sigma}/2$ with $\epsilon^{0123} = 1$. For the QCD axion model, the coupling constant is given by [26]

$$g_{a\gamma\gamma} = \frac{\alpha}{2\pi f_a}\left(\frac{E}{N} - 1.92\right) = \left(0.203\frac{E}{N} - 0.39\right)\frac{m_a}{\mathrm{GeV}^2}, \tag{2}$$

where m_a is the axion mass. E and N are electromagnetic and color anomalies associated with axion axial current, which takes a variety of values [27–33], and E/N are from 5/3 to 44/3. Other than those, there are models whose values are different from the band [34–39]. For ALP, however, $g_{a\gamma\gamma}$ becomes a free parameter. We assume dark matter to consist only of axions and focus on axions of mass $\sim 10 - 100$ meV. To satisfy the observed energy density of dark matter, the number of dark matter particles within the de Broglie wavelength is enormous; their wave functions overlap and can be treated as a classical wave [40]. Then, the amplitude of the axion field is given by

$$a(t) = \frac{\sqrt{2\rho_{\mathrm{DM}}}}{m_{\mathrm{DM}}}\cos(m_{\mathrm{DM}}t + \phi_{\mathrm{DM}}), \tag{3}$$

where m_{DM} is the dark matter mass ($= m_a$) and ϕ_{DM} is the phase of the dark matter field. When we apply a static magnetic field B_0, the electric field is induced by the axion through the interaction given by Eq. (1); it has the same direction as the magnetic field, while the amplitude is given by

$$\begin{aligned} E_{\mathrm{DM}} &= g_{a\gamma\gamma}B_0\frac{\sqrt{2\rho_{\mathrm{DM}}}}{m_{\mathrm{DM}}} \\ &\simeq 7.9\times 10^{-12}\,\frac{\mathrm{V}}{\mathrm{m}}\left(\frac{g_{a\gamma\gamma}}{10^{-11}\ \mathrm{GeV}^{-1}}\right)\left(\frac{B_0}{1\ \mathrm{T}}\right) \\ &\quad\times\left(\frac{m_{\mathrm{DM}}}{1\ \mathrm{meV}}\right)^{-1}\left(\frac{\rho_{\mathrm{DM}}}{0.45\ \mathrm{GeVcm}^{-3}}\right)^{\frac{1}{2}}. \end{aligned} \tag{4}$$

The shift current is regarded as a second-order DC response and can be expressed in terms of the integral over the shift of the Berry connection over the Brillouin zone and is directly related to the shift of the center of mass of electron states [41]. Indeed, the same effect can also be observed with a small frequency current as well [42]. In this Letter, we also call it simply shift current and will apply it for axion signal broadband search. By formulating a coherent state path integral formalism for an electronic system at finite temperature, we derive the general response up to the second order with general electric fields. Details of the derivation are provided in the appendix A-D. With general input electric field $\boldsymbol{E}(t) = \int d\omega\, e^{-i\omega t}\boldsymbol{E}(\omega)$, the shift current with small frequency ω is given by

$$\begin{aligned} \langle \widehat{J}^{\mu}_{\mathrm{shift}}\rangle^{(2)}(\omega) =\ & \frac{1}{2}\sum_{ab}\int\frac{d^d\boldsymbol{k}}{(2\pi)^d}\int d\omega_1 d\omega_2\left(\frac{-e^3}{\omega_1\omega_2}\right) \\ &\times E^{\alpha_1}(\omega_1)E^{\alpha_2}(\omega_2)\delta(\omega-\omega_1-\omega_2) \\ &\times r^{\mu\alpha_1}_{\boldsymbol{k}ab}r^{\alpha_2}_{\boldsymbol{k}ba}\left(\frac{f_{ab}}{\omega_2-\varepsilon_{\boldsymbol{k}ba}+i\gamma}\right) + (\alpha_1,\omega_1\leftrightarrow\alpha_2,\omega_2), \end{aligned} \tag{5}$$

where

$$r^{\mu}_{\boldsymbol{k}ab} = i\varepsilon_{\boldsymbol{k}ab}\mathcal{A}^{\mu}_{ab}(\boldsymbol{k}), \tag{6}$$

$$r^{\mu\alpha}_{\boldsymbol{k}ab} = \left[\partial_{k_\mu}r^{\alpha}_{\boldsymbol{k}ab} - i\left(\mathcal{A}^{\mu}_{aa}(\boldsymbol{k}) - \mathcal{A}^{\mu}_{bb}(\boldsymbol{k})\right)r^{\alpha}_{\boldsymbol{k}ab}\right], \tag{7}$$

with the Berry connection defined by

$$\mathcal{A}^{\mu}_{ab}(\boldsymbol{k}) \equiv i\langle u_{\boldsymbol{k}a}|\frac{\partial}{\partial k_\mu}|u_{\boldsymbol{k}b}\rangle_V. \tag{8}$$

The integration over $\boldsymbol{k}$ in Eq. (5) is for the Brillouin zone. The state $|u_{\boldsymbol{k}a}\rangle$ is the Bloch state of the energy level a with momentum $\boldsymbol{k}$, $\varepsilon_{\boldsymbol{k}ab} \equiv \varepsilon_{\boldsymbol{k}a} - \varepsilon_{\boldsymbol{k}b}$ with $\varepsilon_{\boldsymbol{k}a}$ denoting the energy level a with momentum $\boldsymbol{k}$, and $f_{ab} \equiv f_a - f_b$ with $f_a = f(\varepsilon_{\boldsymbol{k}a})$ denoting the Fermi-Dirac distribution of electron in $\varepsilon_{\boldsymbol{k}a}$. The subscript V in Eq. (8) means that the spatial integration over the wave function is performed within one unit cell. The energy conservation law is reflected in the delta function $\delta(\omega-\omega_1-\omega_2)$. Phenomenologically, to take into account the electron scattering effect in the material, we replaced ω_i for $\omega_i + i\gamma$, where γ is determined by the scattering rate [43]. To derive Eq. (5), we also assumed γ, ω are sufficiently small compared to the energy scale of the system. Throughout this Letter, we consider the time-reversal symmetry material with broken spatial-inversion symmetry. Given that the material has broken spatial-inversion symmetry, the center of the wave function of electronic states can be non-zero and different from each other. (We comment that the center of an electron wave function can be given by the integration of the Berry connection over the Brillouin zone. See, e.g., Eq. (B11) in Appendix B or Ref. [41].) The non-zero shift current can be obtained provided that $\omega_{1,2}$ reside in the range of energy gap covered by the band structure of the material, i.e., there is

$\boldsymbol{k}$ in Brillouin zone satisfying $\varepsilon_{\boldsymbol{k}ba} \simeq \omega_{1,2}$ for an arbitrary pair (a, b). Then, the resonant transition between two states occurs, generating a shift current. We note that the integration over $\boldsymbol{k}$ would (approximately) cancel the γ dependence of the conductivity if the band structure is wide, giving the robustness of the shift current against an impurity of the system and frequency fluctuation. This is one of the characteristics of shift current, making it a promising way of detecting optical signals. With the time-reversal symmetry condition, the intrinsic second-order response other than the shift current is purely circular and becomes zero for a linearly polarized field. We assume that the shift current (Eq. (5)) is the dominant contribution among the second-order processes.

In our strategy, to enhance and detect a feeble dark matter field, we apply another electric field $E_{\rm exp}$ and detect the cross-term of the shift-current response ($J \propto E_{\rm DM}E_{\rm exp}$). Then, a sizable output current is generated by applying high power $E_{\rm exp}$. In total, the external electric field is given by

$$E(t) = \mathrm{Re}\left[E_{\rm DM}e^{im_{\rm DM}t - i\phi_{\rm DM}} + E_{\rm exp}e^{-i\omega_{\rm exp}t}\right], \qquad (9)$$

where, for convenience, we set the sign of the exponent oppositely and assume $m_{\rm DM}, \omega_{\rm exp} > 0$ without loss of generality. Then, the output shift current has frequency $\Delta\omega = -m_{\rm DM} + \omega_{\rm exp}$. We read out the relevant output current of the form :

$$\langle \widehat{J}^{\mu} \rangle^{(2)}_{\rm shift}(\Delta\omega) = \sigma^{\mu\alpha_1\alpha_2}_{\rm shift}(\Delta\omega) E^{\alpha_1}_{\rm DM} e^{-i\phi_{\rm DM}} E^{\alpha_2}_{\rm exp}, \qquad (10)$$

where $\sigma^{\mu\alpha_1\alpha_2}_{\rm shift}(\Delta\omega)$ is the shift current conductivity. The conductivity reads

$$\sigma^{\mu\alpha_1\alpha_2}_{\rm shift}(\Delta\omega) = \sum_{ab} \int \frac{d^d\boldsymbol{k}}{(2\pi)^d} \left(\frac{e^3}{m_{\rm DM}\omega_{\rm exp}}\right) \times f_{ab}\left[\frac{r^{\mu\alpha_1}_{\boldsymbol{k}ab} r^{\alpha_2}_{\boldsymbol{k}ba}}{m_{\rm DM} - \varepsilon_{\boldsymbol{k}ba} + i\gamma} - \frac{r^{\mu\alpha_2}_{\boldsymbol{k}ba} r^{\alpha_1}_{\boldsymbol{k}ab}}{\omega_{\rm exp} - \varepsilon_{\boldsymbol{k}ba} + i\gamma}\right]. \qquad (11)$$

The typical energy scale of electronic bands is $\sim \mathcal{O}(100)$ THz. We consider applying $\omega_{\rm exp} \sim O(100)$ THz and focus on current output with frequency $\Delta\omega \lesssim \mathcal{O}(1)$ THz. With this condition, the resonant transition of an electron can occur, and Eq. (11) is well approximated. Also, the output signal can be easily detected compared to the original source. The signal linewidth is determined by that of $E_{\rm DM}$ and $E_{\rm exp}$. We take the linewidth of $E_{\rm exp}$ and $E_{\rm DM}$ as $\Delta\omega_{\rm exp} = 10$ GHz [44] and $\Delta m_{\rm DM} \simeq m_{\rm DM}v^2_{\rm DM} \simeq 0.1$ GHz, respectively, where we assume dark matter velocity $v_{\rm DM} \simeq 10^{-3}$. Therefore, we expect the linewidth of the signal to be $\sigma_{\rm sig} \sim \max\{\Delta m_{\rm DM}, \Delta\omega_{\rm exp}\} \simeq 10$ GHz.

Our method for axion search can be performed in a broadband manner. We illustrate this property considering conductivity $\sigma^{(\rm 1D,2band)}_{\rm shift}$ in a two-band system with a 1D Rice-Mele Hamiltonian as a toy model. The system consists of two types of ions as a unit cell aligned repeatedly in a 1-dimensional line, and the electron state

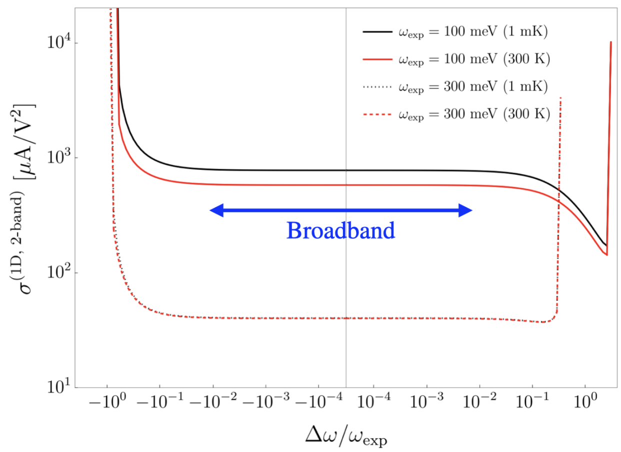

FIG. 1. The plot of the shift-current conductivity as a function of $\Delta\omega/\omega_{\rm exp}$ with fixed frequency $\omega_{\rm exp}$ of 1D Rice-Mele model. We illustrate the characteristics of the response with two fields of the 2-band system. We set the energy gap covering 30 meV to 400 meV depending on momentum k. The conductivities are derived with $T = 1$ mK and $T = 300$ mK with the Fermi energy lying at the middle of the two bands. The divergent values on the edge come from the points where the group velocity vanishes.

is described by a tight-binding model. The model has two energy bands of electron states, where we set an energy gap covering 30 meV to 400 meV depending on momentum k, while the spatial inversion symmetry is broken by a difference in electron potential between two ions in the unit cell (see appendix E for detail).

The shift-current conductivity as a function of $\Delta\omega/\omega_{\rm exp}$ with fixed frequency $\omega_{\rm exp}$ is shown in FIG. 1. In the plot, we directly use Eq. (11), however, it should be kept in mind that the equation is reliable for $\Delta\omega \lesssim \omega_{\rm exp}$. It is of importance that the response amplitude is almost the same for small $\Delta\omega \ll \omega_{\rm exp}$. Also, the search width is not determined by the scattering rate γ as in the usual resonance experiment, but directly by the band structure. This is because the resonant transition is always automatically ensured by integration over $\boldsymbol{k}$ in Eq. (11) provided that the source has a frequency that matches the band gap for an arbitrary k in the Brillouin zone.

We exemplify TaAs as a real material setup. TaAs is a Type-I Weyl semimetal that lacks inversion symmetry and supports a bulk photovoltaic effect. In a 3D system, the breaking of spatial inversion symmetry can generally lead to the appearance of degenerate Weyl nodes that host gapless excitations with topological stability [45]. The Weyl semimetal TaAs possesses 24 Weyl nodes throughout the Brillouin zone. Since TaAs has C_{4v} symmetry, the xxx component of the current conductivity σ^{xxx} is identically zero due to the mirror symmetry with yz plane, while the xzx component σ^{xzx} has a non-zero contribution [46]. This directional property of material provides the great benefit that we can carefully choose the direction of the input electric field and magnetic field

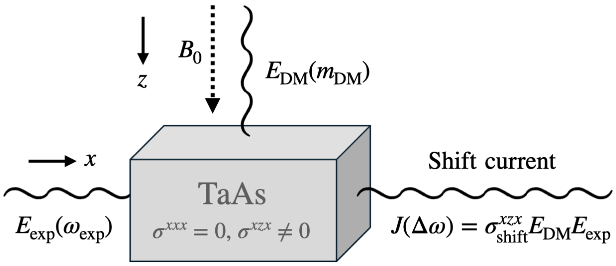

FIG. 2. The schematic picture of the experimental setup. The static magnetic field B_0 converts axion to photon $E_{\rm DM}$. In a Type-I Weyl semimetal TaAs, the second order response of $E_{\rm DM}$ and $E_{\rm exp}$ generates the output signal J. We look for the axion dark matter satisfying the condition $\Delta\omega = -m_{\rm DM} + \omega_{\rm exp}$ where $\Delta\omega$ is a small frequency difference. Since $\sigma^{xxx} = 0$, $\sigma^{xzx}_{\rm shift} \neq 0$, the background shift current $J_{\rm BG} = \sigma^{xxx} E_{\rm exp} E_{\rm exp}$ vanishes.

such that the background current from the experimental field $J_{\rm BG} \propto E_{\rm exp}E_{\rm exp}$ vanishes. In FIG. 2, we show the schematic picture of the experimental setup. We apply a static magnetic field B_0 in the z direction, which converts axion to photon $E_{\rm DM} \parallel z$. We also apply an oscillating electric field $E_{\rm exp}$ in the x direction. Measuring the output current in the x direction, we detect the axion-induced shift current $J = \sigma^{xzx}_{\rm shift} E_{\rm DM} E_{\rm exp}$. In this setup, the background second-order response $J_{\rm BG} = \sigma^{xxx} E_{\rm exp} E_{\rm exp}$ vanishes. One should also consider the general background other than the second-order response that might be generated from the experimental field $E_{\rm exp}$. Indeed, the mirror symmetry with yz plane also forbids all of the even-order responses in the x direction, so we can neglect the background with a frequency similar to that of the signal. On the other hand, the other currents from general odd-order responses, have a frequency at least $\omega_{\rm exp}$, which is far from the signal, so they can also be neglected.

The shift-current conductivity is observed to be $\sigma^{xzx}_{\rm shift} \sim 200\ \mu{\rm A/V}^2$ with input field with frequency around 100 meV, while it is expected to be in the range $100 - 2000\ \mu{\rm A/V}^2$ with input field's frequency range $25 - 350$ meV (See [47] and its supplemental material). For convenience, we assume that two input fields $(E_{\rm exp}, E_{\rm DM})$ with frequencies within the range give the shift-current conductivity of $\sim 200\ \mu{\rm A/V}^2$ in our calculation of the sensitivity of axion detection.

III. PROTOCOL & SENSITIVITY

To estimate the sensitivity, we need to take into account the effect of the dark matter phase $\phi_{\rm DM}$. We treat the electric fields $E_{\rm DM}, E_{\rm exp}$ as a coherently oscillating classical field with a small fluctuation $\Delta m_{\rm DM}$, $\Delta\omega_{\rm exp}$. If the measurement time τ is as large as $\Delta m_{\rm DM}\tau \sim 1$ $(\Delta\omega_{\rm exp}\tau \sim \mathcal{O}(1))$, the phase of the axion field (experimental field) varies, and the system loses phase information. This timescale is called "coherence time", within which we can treat the signal as coherently oscillating. We set τ to be $\min\{1/\Delta\omega_{\rm exp}, 1/\Delta m_{\rm DM}\} \simeq 0.1$ ns so that, within one cycle of measurement, the signal coherently oscillates and the phase $\phi_{\rm DM}$ can be treated as constant (but random for each measurement). In addition, dark matter also has spatial fluctuations and the corresponding coherence length scale is $\lambda_{\rm De-Broglie} = 1/(m_{\rm DM}v_{\rm DM}) \simeq \mathcal{O}(1)$ cm. We then set an experimental length scale $L_{\rm exp}$ to be $\mathcal{O}(1)$ cm.

The following is the procedure for signal collection for sensitivity estimation:

1. We apply an oscillating electric field $E_{\rm exp}$ and magnetic field B_0 to the system and record the time evolution of the output current.

2. For each time interval $\tau = 0.1$ ns, we Fourier transform the data and read out signal power $P_{\rm sig}$ at the chosen frequency $\Delta\omega$. (Practically, this might be done using a spectral analyzer or heterodyne receiver.) We take the resolution bandwidth or bin's width as $\Delta f_{\rm bin} \sim \sigma_{\rm sig} = 10$ GHz. Importantly, we can probe many bins simultaneously; the detectable response frequency $\Delta\omega$ is broadband covering from 0 Hz to ~ 1 THz. We denote this range as $\Delta f_{\rm scan} = 1$ THz and the interrogation time for this range as $\tau_{\rm scan}$.

3. We change $\omega_{\rm exp}$ to several values or sweep it during the experiment so that the desired scan range of $\omega_{\rm DM}$ is achieved. Using several values of $\omega_{\rm exp}$ is necessary to distinguish the sign of $\Delta\omega$.

The theoretical prediction of the averaged current signal power for each bin is

$$\langle P_{\rm sig}\rangle = \frac{1}{2} R_{\rm exp} |\sigma^{xzx}_{\rm shift}|^2 E^2_{\rm DM} E^2_{\rm exp} L^4_{\rm exp} \tag{12}$$

$$= 6.2\times 10^{-15}\ \mu{\rm W} \left(\frac{R_{\rm exp}}{50\ \Omega}\right)\left(\frac{\sigma^{xzx}_{\rm shift}}{200\ \mu{\rm A/V}^2}\right)^2 \times\left(\frac{g_{a\gamma\gamma}}{10^{-11}\ {\rm GeV}^{-1}}\right)^2\left(\frac{B_0}{1\ {\rm T}}\right)^2\left(\frac{m_{\rm DM}}{1\ {\rm meV}}\right)^{-2} \times\left(\frac{\rho_{\rm DM}}{0.45\ {\rm GeVcm}^{-3}}\right)\left(\frac{E_{\rm exp}}{10^8\ {\rm V/m}}\right)^2\left(\frac{L_{\rm exp}}{1\ {\rm cm}}\right)^4, \tag{13}$$

where $R_{\rm exp}$ is the resistance of the conductor for collecting the current and $L_{\rm exp}$ is the length scale of the sample. Note that the randomness of the relative phase $\phi_{\rm DM}$ of each measurement is taken into account as the factor 1/2 in front. We suppose that the main noise comes from Johnson-Nyquist noise [48, 49] of the outside system used to probe the current signal. Then, Signal to Noise Ratio (SNR) for each bin of $\omega_{\rm DM}$ is obtained by the radiometer equation [50] as

$${\rm SNR} = \frac{\langle P_{\rm sig}\rangle}{4k_{\rm B}T}\sqrt{\frac{\tau_{\rm scan}}{\Delta f_{\rm bin}}}. \tag{14}$$

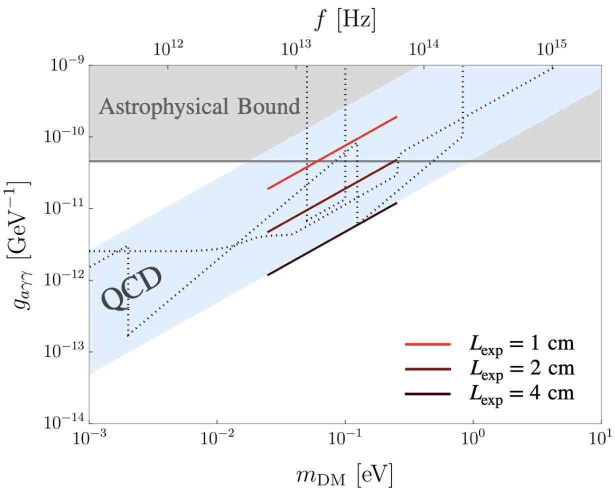

FIG. 3. Sensitivity to the axion photon coupling $g_{a\gamma\gamma}$ determined by Signal to Noise Ratio (SNR) assuming TaAs as a sample. The dotted lines represent the other experimental proposals (IAXO [51–53], BREAD [54] and WISPFI [55]). The blue band corresponds to the allowed region of the QCD axion. We assumed a static magnetic field $B_0 = 1$ T and oscillating electric field $E_{\rm exp} = 10^8$ V/m. The total observation time is 100 days.

We show the expected sensitivity of TaAs determined by SNR = 1 in FIG. 3 where we used $B_0 = 1$ T, $E_{\rm exp} = 10^8$ V/m (referenced from the experiment applying THz pulse laser [56]), $T = 1$ mK, $R_{\rm exp} = 50\ \Omega$, $\Delta f_{\rm scan} = 1$ THz and $\tau_{\rm scan} = 1$ day. To cover the detectable range (10 meV - 300 meV) determined by the material TaAs band structure, we require a total observation time of (100 THz/$\Delta f_{\rm scan}$) $\simeq$100 days.

The gray dotted lines represent the prospects of other experiments (IAXO [51–53], BREAD [54] and WISPFI [55]). The blue band corresponds to the allowed region of QCD Axion, which is covered by the TaAs detector with area $L_{\rm exp} \times L_{\rm exp} \sim 4 \times 4$ cm^2.

IV. DISCUSSION AND CONCLUSION

In this work, we have proposed a novel method to probe axion dark matter using the shift current in topological materials, in combination with difference frequency generation. In the presence of a magnetic field, axions can convert to photons, and the application of an oscillating electric field can enhance the resulting signal through the second-order nonlinear response of the shift current. Using difference frequency generation, we can probe the mass range of $\mathcal{O}(10) - \mathcal{O}(100)$ meV with the output signal frequency reduced to DC or below $\mathcal{O}(1)$ THz. We demonstrate that with the input oscillating electric field of 10^8 V/m strength and static magnetic field of 1 T, the axion dark matter can be probed down to the parameter $g_{a\gamma\gamma} \sim 10^{-12}$ GeV^{-1} covering the parameter region of QCD axion, using type-I Weyl semimetal material TaAs using a total observation time of 100 days.

One challenge lies in the application of the experimental electric field. The assumed oscillating field strength for the signal enhancement, on the order of 10^8 V/m, is currently achievable using short-pulse laser technology. Indeed, the shift current response is fast and would fully develop with a time scale $\mathcal{O}(10)$ - $\mathcal{O}(100)$ fs, determined by the material relaxation rate [57, 58]. However, we still need a long enough pulse with time at least 100 ps to collect enough data for the desired resolution bandwidth of 10 GHz.

In this paper, we adopt the ferroelectric material as a sample to discuss axion sensitivity with our method. In addition to electronic excitations, the shift current response can also occur through quasiparticle excitations below the electronic band gap, including magnon [59, 60] or phonon excitations [61], such as in perovskite manganite [62] and $BaTiO_3$ [63], respectively. These kinds of excitation have an energy scale of $0.1 - 1$ meV (~ 10 GHz), and might be used to conveniently probe the smaller axion mass range compared to the case of using electronic excitation. Also, in principle, we might apply the same proposed method for probing hidden photons, another candidate of dark matter, by using an oscillating electric field to enhance the shift current induced by dark photons.

Acknowledgments: We gratefully thank Masashi Kawasaki for discussions at an earlier stage of this work. Also, Koichi Hamaguchi and Takeo Moroi for reading and giving comments on the draft. This work is partially supported by JST SPRING, Grant Number JPMJSP2108, JSPS KAKENHI Grant Number 24KJ0713, JSPS KAKENHI Grant Number 25KJ0950, and JSPS KAKENHI Grant Number 23KJ0678.

[1] S. Weinberg, A New Light Boson?, Phys. Rev. Lett. **40**, 223 (1978).
[2] F. Wilczek, Problem of Strong P and T Invariance in the Presence of Instantons, Phys. Rev. Lett. **40**, 279 (1978).
[3] R. D. Peccei and H. R. Quinn, CP Conservation in the Presence of Instantons, Phys. Rev. Lett. **38**, 1440 (1977).
[4] E. Witten, Some Properties of O(32) Superstrings, Phys. Lett. B **149**, 351 (1984).
[5] J. P. Conlon, The QCD axion and moduli stabilisation, JHEP **05**, 078, arXiv:hep-th/0602233.
[6] P. Svrcek and E. Witten, Axions In String Theory, JHEP **06**, 051, arXiv:hep-th/0605206.
[7] A. Arvanitaki, S. Dimopoulos, S. Dubovsky, N. Kaloper, and J. March-Russell, String Axiverse, Phys. Rev. D **81**, 123530 (2010), arXiv:0905.4720 [hep-th].
[8] M. Cicoli, M. Goodsell, and A. Ringwald, The type IIB

string axiverse and its low-energy phenomenology, JHEP **10**, 146, arXiv:1206.0819 [hep-th].

[9] J. E. Kim and G. Carosi, Axions and the Strong CP Problem, Rev. Mod. Phys. **82**, 557 (2010), [Erratum: Rev.Mod.Phys. 91, 049902 (2019)], arXiv:0807.3125 [hep-ph].

[10] P. Arias, D. Cadamuro, M. Goodsell, J. Jaeckel, J. Redondo, and A. Ringwald, WISPy Cold Dark Matter, JCAP **06**, 013, arXiv:1201.5902 [hep-ph].

[11] M. Kawasaki and K. Nakayama, Axions: Theory and Cosmological Role, Ann. Rev. Nucl. Part. Sci. **63**, 69 (2013), arXiv:1301.1123 [hep-ph].

[12] D. J. E. Marsh, Axion Cosmology, Phys. Rept. **643**, 1 (2016), arXiv:1510.07633 [astro-ph.CO].

[13] L. Di Luzio, M. Giannotti, E. Nardi, and L. Visinelli, The landscape of QCD axion models, Phys. Rept. **870**, 1 (2020), arXiv:2003.01100 [hep-ph].

[14] C. A. J. O'Hare, Cosmology of axion dark matter, PoS **COSMICWISPers**, 040 (2024), arXiv:2403.17697 [hep-ph].

[15] E. G. M. Ferreira, Ultra-light dark matter, Astron. Astrophys. Rev. **29**, 7 (2021), arXiv:2005.03254 [astro-ph.CO].

[16] B. R. Safdi, TASI Lectures on the Particle Physics and Astrophysics of Dark Matter, PoS **TASI2022**, 009 (2024), arXiv:2303.02169 [hep-ph].

[17] P. Sikivie, Experimental Tests of the Invisible Axion, Phys. Rev. Lett. **51**, 1415 (1983), [Erratum: Phys.Rev.Lett. 52, 695 (1984)].

[18] P. Sikivie, Experimental tests of the "invisible" axion, Phys. Rev. Lett. **51**, 1415 (1983).

[19] E. Fatuzzo, G. Harbeke, W. J. Merz, R. Nitsche, H. Roetschi, and W. Ruppel, Ferroelectricity in sbsi, Phys. Rev. **127**, 2036 (1962).

[20] V. Fridkin, I. Groshik, V. Lakhovizkaya, M. Mikhailov, and V. Nosov, Current saturation and photoferroelectric effect in sbsi, Applied Physics Letters **10**, 354 (1967).

[21] W. T. H. Koch, R. Munser, W. Ruppel, and P. W. and, Anomalous photovoltage in batio3, Ferroelectrics **13**, 305 (1976), https://doi.org/10.1080/00150197608236596.

[22] P. Ghosez, X. Gonze, P. Lambin, and J.-P. Michenaud, Born effective charges of barium titanate: Band-by-band decomposition and sensitivity to structural features, Physical Review B **51**, 6765 (1995).

[23] N. Ogawa, M. Sotome, Y. Kaneko, M. Ogino, and Y. Tokura, Shift current in the ferroelectric semiconductor sbsi, Phys. Rev. B **96**, 241203 (2017).

[24] M. Sotome, M. Nakamura, J. Fujioka, M. Ogino, Y. Kaneko, T. Morimoto, Y. Zhang, M. Kawasaki, N. Nagaosa, Y. Tokura, *et al.*, Spectral dynamics of topological shift-current in ferroelectric semiconductor sbsi, arXiv preprint arXiv:1801.10297 (2018).

[25] H. Hatada, M. Nakamura, M. Sotome, Y. Kaneko, N. Ogawa, T. Morimoto, Y. Tokura, and M. Kawasaki, Defect tolerant zero-bias topological photocurrent in a ferroelectric semiconductor, Proceedings of the National Academy of Sciences **117**, 20411 (2020), https://www.pnas.org/doi/pdf/10.1073/pnas.2007002117.

[26] G. Grilli di Cortona, E. Hardy, J. Pardo Vega, and G. Villadoro, The QCD axion, precisely, JHEP **01**, 034, arXiv:1511.02867 [hep-ph].

[27] A. R. Zhitnitsky, On Possible Suppression of the Axion Hadron Interactions. (In Russian), Sov. J. Nucl. Phys. **31**, 260 (1980).

[28] M. Dine, W. Fischler, and M. Srednicki, A Simple Solution to the Strong CP Problem with a Harmless Axion, Phys. Lett. B **104**, 199 (1981).

[29] J. E. Kim, Weak Interaction Singlet and Strong CP Invariance, Phys. Rev. Lett. **43**, 103 (1979).

[30] M. A. Shifman, A. I. Vainshtein, and V. I. Zakharov, Can Confinement Ensure Natural CP Invariance of Strong Interactions?, Nucl. Phys. B **166**, 493 (1980).

[31] J. E. Kim, Constraints on very light axions from cavity experiments, Phys. Rev. D **58**, 055006 (1998), arXiv:hep-ph/9802220.

[32] L. Di Luzio, F. Mescia, and E. Nardi, Redefining the Axion Window, Phys. Rev. Lett. **118**, 031801 (2017), arXiv:1610.07593 [hep-ph].

[33] L. Di Luzio, F. Mescia, and E. Nardi, Window for preferred axion models, Phys. Rev. D **96**, 075003 (2017), arXiv:1705.05370 [hep-ph].

[34] M. Farina, D. Pappadopulo, F. Rompineve, and A. Tesi, The photo-philic QCD axion, JHEP **01**, 095, arXiv:1611.09855 [hep-ph].

[35] P. Agrawal, J. Fan, M. Reece, and L.-T. Wang, Experimental Targets for Photon Couplings of the QCD Axion, JHEP **02**, 006, arXiv:1709.06085 [hep-ph].

[36] A. Hook, Solving the Hierarchy Problem Discretely, Phys. Rev. Lett. **120**, 261802 (2018), arXiv:1802.10093 [hep-ph].

[37] L. Di Luzio, B. Gavela, P. Quilez, and A. Ringwald, An even lighter QCD axion, JHEP **05**, 184, arXiv:2102.00012 [hep-ph].

[38] A. V. Sokolov and A. Ringwald, Photophilic hadronic axion from heavy magnetic monopoles, JHEP **06**, 123, arXiv:2104.02574 [hep-ph].

[39] J. Diehl and E. Koutsangelas, Dine-Fischler-Srednicki-Zhitnitsky-type axions and where to find them, Phys. Rev. D **107**, 095020 (2023), arXiv:2302.04667 [hep-ph].

[40] J. W. Foster, N. L. Rodd, and B. R. Safdi, Revealing the Dark Matter Halo with Axion Direct Detection, Phys. Rev. D **97**, 123006 (2018), arXiv:1711.10489 [astro-ph.CO].

[41] T. Morimoto, S. Kitamura, and N. Nagaosa, Geometric aspects of nonlinear and nonequilibrium phenomena, Journal of the Physical Society of Japan **92**, 10.7566/jpsj.92.072001 (2023).

[42] F. de Juan, Y. Zhang, T. Morimoto, Y. Sun, J. E. Moore, and A. G. Grushin, Difference frequency generation in topological semimetals, Physical Review Research **2**, 10.1103/physrevresearch.2.012017 (2020).

[43] D. E. Parker, T. Morimoto, J. Orenstein, and J. E. Moore, Diagrammatic approach to nonlinear optical response with application to weyl semimetals, Physical Review B **99**, 045121 (2019).

[44] T.-T. Lin, L. Wang, K. Wang, T. Grange, S. Birner, and H. Hirayama, Over one watt output power terahertz quantum cascade lasers by using high doping concentration and variable barrier-well height, physica status solidi (RRL)–Rapid Research Letters **16**, 2200033 (2022).

[45] N. Nagaosa, T. Morimoto, and Y. Tokura, Transport, magnetic and optical properties of weyl materials, Nature Reviews Materials **5**, 621 (2020).

[46] B. I. Sturman and V. M. Fridkin, *Photovoltaic and Photorefractive Effects in Noncentrosymmetric Materials*, Ferroelectricity and Related Phenomena, Vol. 12 (Taylor & Francis, London, 1992).

[47] G. B. Osterhoudt, L. K. Diebel, M. J. Gray, X. Yang, J. Stanco, X. Huang, B. Shen, N. Ni, P. J. Moll, Y. Ran,

et al., Colossal mid-infrared bulk photovoltaic effect in a type-i weyl semimetal, Nature materials **18**, 471 (2019).

[48] J. B. Johnson, Thermal agitation of electricity in conductors, Physical review **32**, 97 (1928).

[49] H. Nyquist, Thermal agitation of electric charge in conductors, Physical review **32**, 110 (1928).

[50] R. H. Dicke, The measurement of thermal radiation at microwave frequencies, Review of Scientific Instruments **17**, 268 (1946), https://pubs.aip.org/aip/rsi/article-pdf/17/7/268/19120701/268_1_online.pdf.

[51] I. G. Irastorza *et al.*, Towards a new generation axion helioscope, JCAP **06**, 013, arXiv:1103.5334 [hep-ex].

[52] E. Armengaud *et al.* (IAXO), Physics potential of the International Axion Observatory (IAXO), JCAP **06**, 047, arXiv:1904.09155 [hep-ph].

[53] S.-F. Ge, K. Hamaguchi, K. Ichimura, K. Ishidoshiro, Y. Kanazawa, Y. Kishimoto, N. Nagata, and J. Zheng, Supernova-scope for the Direct Search of Supernova Axions, JCAP **11**, 059, arXiv:2008.03924 [hep-ph].

[54] J. Liu *et al.* (BREAD), Broadband Solenoidal Haloscope for Terahertz Axion Detection, Phys. Rev. Lett. **128**, 131801 (2022), arXiv:2111.12103 [physics.ins-det].

[55] J. M. Batllori, Y. Gu, D. Horns, M. Maroudas, and J. Ulrichs, Searching for weakly interacting sub-eV particles with a fiber interferometer in a strong magnetic field, Phys. Rev. D **109**, 123001 (2024), arXiv:2305.12969 [hep-ex].

[56] Y. Sanari, T. Otobe, Y. Kanemitsu, and H. Hirori, Modifying angular and polarization selection rules of high-order harmonics by controlling electron trajectories in k-space, Nature Communications **11**, 3069 (2020).

[57] F. He, D. Chen, X. Ren, S. Meng, and L. He, Ultrafast shift current dynamics in ws 2 monolayer, Physical Review Research **6**, 013123 (2024).

[58] M. Sotome, M. Nakamura, J. Fujioka, M. Ogino, Y. Kaneko, T. Morimoto, Y. Zhang, M. Kawasaki, N. Nagaosa, Y. Tokura, *et al.*, Spectral dynamics of shift current in ferroelectric semiconductor sbsi, Proceedings of the National Academy of Sciences **116**, 1929 (2019).

[59] T. Morimoto and N. Nagaosa, Shift current from electromagnon excitations in multiferroics, Physical Review B **100**, 235138 (2019).

[60] T. Morimoto, S. Kitamura, and S. Okumura, Electric polarization and nonlinear optical effects in noncentrosymmetric magnets, Phys. Rev. B **104**, 075139 (2021).

[61] T. Morimoto and N. Nagaosa, Direct current generation by dielectric loss in ferroelectrics, Phys. Rev. B **110**, 045129 (2024).

[62] M. Ogino, Y. Okamura, K. Fujiwara, T. Morimoto, N. Nagaosa, Y. Kaneko, Y. Tokura, and Y. Takahashi, Terahertz photon to dc current conversion via magnetic excitations of multiferroics, Nature Communications **15**, 4699 (2024).

[63] Y. Okamura, T. Morimoto, N. Ogawa, Y. Kaneko, G.-Y. Guo, M. Nakamura, M. Kawasaki, N. Nagaosa, Y. Tokura, and Y. Takahashi, Photovoltaic effect by soft phonon excitation, Proceedings of the National Academy of Sciences **119**, e2122313119 (2022).

[64] J. W. Negele and H. Orland, *Quantum Many-Particle Systems*, Frontiers in Physics (Addison-Wesley, Redwood City, CA, 1988).

[65] K. W. Kim, T. Morimoto, and N. Nagaosa, Shift charge and spin photocurrents in dirac surface states of topological insulator, Physical Review B **95**, 035134 (2017).

Appendix A: Path integral formalism in quantum many-particle systems

In this section, we summarize the path integral formulation for quantum many-particle systems[64].

1. Notation

Let us begin with the second quantized Hamiltonian for electrons.

$$\widehat{H}_0 = \sum_a \int \frac{d^d \boldsymbol{k}}{(2\pi)^d} \varepsilon_{\boldsymbol{k}a} c^\dagger_{\boldsymbol{k}a} c_{\boldsymbol{k}a} \tag{A1}$$

where $\{a\}$ is the band label. The integration over k is for the Brillouin zone. $\varepsilon_{\boldsymbol{k}a}$ is the eigen energy and $c^\dagger_{\boldsymbol{k}a},\ c_{\boldsymbol{k}n}$ are the corresponding creation/annihilation operators satisfying the anti-commutation relation:

$$\{c_{\boldsymbol{k}a},\ c^\dagger_{\boldsymbol{k}'a'}\} = (2\pi)^d \delta_{aa'} \delta^d(\boldsymbol{k}-\boldsymbol{k}'),\ \ \{c_{\boldsymbol{k}a},\ c_{\boldsymbol{k}'a'}\} = \{c^\dagger_{\boldsymbol{k}a},\ c^\dagger_{\boldsymbol{k}'a'}\} = 0. \tag{A2}$$

Vacuum state $|0\rangle$ is defined by annihilation operators,

$$c_{\boldsymbol{k}a}|0\rangle \equiv 0. \tag{A3}$$

One electron state is defined by creation operators,

$$|\psi_{\boldsymbol{k}a}\rangle \equiv c^\dagger_{\boldsymbol{k}a}|0\rangle. \tag{A4}$$

Using position state $|\boldsymbol{r}\rangle$, position representation of the wave function is defined by,

$$\psi_{\boldsymbol{k}a}(\boldsymbol{r}) \equiv \langle \boldsymbol{r}|\psi_{\boldsymbol{k}a}\rangle. \tag{A5}$$

2. Fermion coherent states

We define the coherent state of a fermion by the eigenstate of annihilation operators,

$$c_\alpha|\xi\rangle = \xi_\alpha|\xi\rangle \tag{A6}$$

where ξ_α are Grassmann numbers[1] and the label α represents general indices. Such state can be realized by,

$$|\xi\rangle = e^{-\sum_\alpha \xi_\alpha c_\alpha^\dagger}|0\rangle = \prod_\alpha (1-\xi_\alpha c_\alpha^\dagger)|0\rangle \tag{A7}$$

If we take the different set of eigenvalues $\{\xi'_\alpha\}$, we can construct the different coherent state $|\xi'\rangle$. The overlap of two coherent states is,

$$\langle\xi|\xi'\rangle = e^{\sum_\alpha \xi^*_\alpha \xi'_\alpha} \tag{A8}$$

The closure relation is written by,

$$\int \prod_\alpha d\xi^*_\alpha d\xi_\alpha e^{-\sum_\alpha \xi^*_\alpha\xi_\alpha}|\xi\rangle\langle\xi| = 1 \tag{A9}$$

For a complete set of states $\{|n\rangle\}$ in the Fock space, the trace of an operator $\widehat{A}$ can be written by,

$$\mathrm{Tr}\,\widehat{A} = \sum_n \langle n|\widehat{A}|n\rangle = \int \prod_\alpha d\xi^*_\alpha d\xi_\alpha e^{-\sum_\alpha \xi^*_\alpha\xi_\alpha}\langle -\xi|\widehat{A}|\xi\rangle \tag{A10}$$

3. Coherent state path integral

Consider the Hamiltonian $\widehat{H}(c_\alpha^\dagger,\ c_\alpha)$ which is written in normal ordering. Then, the matrix element of the time evolution operator is

$$\langle\xi_f|e^{-\frac{i}{\hbar}\widehat{H}(t_f-t_i)}|\xi_i\rangle = \int_{\xi_\alpha(t_i)=\xi_{\alpha,i}}^{\xi_\alpha(t_f)=\xi_{\alpha,f}} \mathcal{D}\xi^*\mathcal{D}\xi\, e^{\sum_\alpha \xi^*_\alpha(t_f)\xi_\alpha(t_f)} \times e^{\frac{i}{\hbar}\int_{t_i}^{t_f} dt\left[\sum_\alpha i\hbar\xi^*_\alpha(t)\frac{\partial\xi_\alpha(t)}{\partial t} - H(\xi^*_\alpha(t),\xi_\alpha(t))\right]} \tag{A11}$$

$$\mathcal{D}\xi^*\mathcal{D}\xi = \lim_{M\to\infty}\prod_{k=1}^{M-1}\prod_\alpha d\xi^*_{\alpha,k}d\xi_{\alpha,k}. \tag{A12}$$

The partition function is defined by,

$$Z \equiv \mathrm{Tr}\, e^{-\beta(\widehat{H}-\mu\widehat{N})}. \tag{A13}$$

We expand it by coherent state with (A10),

$$Z = \int \prod_\alpha d\xi^*_\alpha d\xi_\alpha e^{-\sum_\alpha \xi^*_\alpha\xi_\alpha}\langle -\xi|e^{-\beta(\widehat{H}-\mu\widehat{N})}|\xi\rangle. \tag{A14}$$

The bracket part is very similar to $\langle\xi_f|e^{-\frac{i}{\hbar}\widehat{H}(t_f-t_i)}|\xi_i\rangle$ in (A11). We transform the preceding expression into the path integral form by performing the following three steps:

- Analytic continuation: the domain of t is extended from the real line to the complex plane.
- Redefinition of variables and fields: $t = -i\tau$ $(t_i = -i\tau_i,\ t_f = -i\tau_f)$, $\xi(\tau) \equiv \xi(t)$.
- Boundary condition: $\tau_i = 0,\ \tau_f = \beta,\ \xi_i = \xi,\ \xi_f = -\xi$.

---

[1] They obey Grassmann algebra:
$\{\xi_\alpha,\ \xi_\beta\} = 0,\ \ \{\xi_\alpha,\ c_\beta^{(\dagger)}\} = 0,\ \ (\xi_\alpha c_\beta)^\dagger = c_\beta^\dagger\xi^*_\alpha$, etc.

Then, (A11) becomes in $\hbar = 1$ unit

$$
\begin{aligned}
&\langle -\xi | e^{-i\widehat{H}(-i\beta-0)} | \xi \rangle \\
&= \int_{\xi_\alpha(\tau_i)=\xi_\alpha}^{\xi_\alpha(\tau_f)=-\xi_\alpha} \mathcal{D}\xi^* \mathcal{D}\xi \, e^{\sum_\alpha (-\xi_\alpha^*)(-\xi_\alpha)} \times e^{i \int_{\tau_i}^{\tau_f} (-id\tau) \left[\sum_\alpha i\xi_\alpha^*(\tau) \frac{\partial \xi_\alpha(\tau)}{-i\partial\tau} - H(\xi_\alpha^*(\tau), \xi_\alpha(\tau)) \right]} \\
&= \int_{\xi_\alpha(\tau_i)=\xi_\alpha}^{\xi_\alpha(\tau_f)=-\xi_\alpha} \mathcal{D}\xi^* \mathcal{D}\xi \, e^{\sum_\alpha \xi_\alpha^* \xi_\alpha} \times e^{- \int_{\tau_i}^{\tau_f} d\tau \left[\sum_\alpha \xi_\alpha^*(\tau) \frac{\partial \xi_\alpha(\tau)}{\partial\tau} + H(\xi_\alpha^*(\tau), \xi_\alpha(\tau)) \right]}.
\end{aligned}
\tag{A15}
$$

Therefore, in the case of $\mu = 0$, the partition function becomes

$$
Z = \int_{\xi_f = -\xi_i} \mathcal{D}\xi^* \mathcal{D}\xi \, e^{- \int_0^\beta d\tau \left[\sum_\alpha \xi_\alpha^*(\tau) \frac{\partial \xi_\alpha(\tau)}{\partial\tau} + H(\xi_\alpha^*(\tau), \xi_\alpha(\tau)) \right]},
\tag{A16}
$$

where $\prod_\alpha d\xi_\alpha^* d\xi_\alpha$ in (A14) is absorbed into $\mathcal{D}\xi^*\mathcal{D}\xi$.

Appendix B: Derivation of the interaction terms

In this section, we derive electromagnetic interaction terms as perturbations.

1. Bloch state

Assuming periodic boundary condition ($r_i \to r_i + L_i$), the wave function can be expressed by

$$\psi_{\boldsymbol{k}a}(\boldsymbol{r}) = e^{i\boldsymbol{k}\cdot\boldsymbol{r}} u_{\boldsymbol{k}a}(\boldsymbol{r}) \tag{B1}$$

where $u_{\boldsymbol{k}a}(\boldsymbol{r})$ is a periodic function:

$$u_{\boldsymbol{k}a}(\boldsymbol{r}) = u_{\boldsymbol{k}a}(\boldsymbol{r} + m_i L_i). \tag{B2}$$

It is an eigenfunction of k-dependent Hamiltonian associated with the operator (A1),

$$\widehat{H}_0(\boldsymbol{k}) \equiv e^{-i\boldsymbol{k}\cdot\widehat{\boldsymbol{r}}} \widehat{H}_0 e^{i\boldsymbol{k}\cdot\widehat{\boldsymbol{r}}}. \tag{B3}$$

General one-particle state can be expanded by the set of eigen functions

$$\Psi = \sum_a \int \frac{d^d\boldsymbol{k}}{(2\pi)^d} C_{\boldsymbol{k}a} |\psi_{\boldsymbol{k}a}\rangle. \tag{B4}$$

2. Covariant derivative

Let us calculate the expectation value of the position operator $\widehat{\boldsymbol{r}}$.

$$\begin{aligned}
\langle \Psi' | \widehat{\boldsymbol{r}} | \Psi \rangle =& \int d^d\boldsymbol{r} \langle \Psi' | \widehat{\boldsymbol{r}} | \boldsymbol{r} \rangle \langle \boldsymbol{r} | \Psi \rangle \\
=& \sum_{a',a} \int d^d\boldsymbol{r} \frac{d^d\boldsymbol{k}'}{(2\pi)^d} \frac{d^d\boldsymbol{k}}{(2\pi)^d} C^*_{\boldsymbol{k}'a'} i e^{-i\boldsymbol{k}'\cdot\boldsymbol{r}} u^*_{\boldsymbol{k}'a'}(\boldsymbol{r}) e^{i\boldsymbol{k}\cdot\boldsymbol{r}} u_{\boldsymbol{k}a}(\boldsymbol{r}) \left(\frac{\partial}{\partial \boldsymbol{k}} C_{\boldsymbol{k}a} \right) \qquad \text{(B5)} \\
&+ \sum_{a',a} \int d^d\boldsymbol{r} \frac{d^d\boldsymbol{k}'}{(2\pi)^d} \frac{d^d\boldsymbol{k}}{(2\pi)^d} C^*_{\boldsymbol{k}'a'} i e^{-i\boldsymbol{k}'\cdot\boldsymbol{r}} e^{i\boldsymbol{k}\cdot\boldsymbol{r}} u^*_{\boldsymbol{k}'a'}(\boldsymbol{r}) \left(\frac{\partial}{\partial \boldsymbol{k}} u_{\boldsymbol{k}a}(\boldsymbol{r}) \right) C_{\boldsymbol{k}a}. \qquad \text{(B6)}
\end{aligned}$$

The first term (B5):

$$\begin{aligned}
\int d^d\boldsymbol{r} e^{-i\boldsymbol{k}'\cdot\boldsymbol{r}} u^*_{\boldsymbol{k}'a'}(\boldsymbol{r}) e^{i\boldsymbol{k}\cdot\boldsymbol{r}} u_{\boldsymbol{k}a}(\boldsymbol{r}) =& \int d^d\boldsymbol{r} \psi^*_{\boldsymbol{k}'a'}(\boldsymbol{r}) \psi_{\boldsymbol{k}a}(\boldsymbol{r}) \\
=& (2\pi)^d \delta_{a'a} \delta(\boldsymbol{k}' - \boldsymbol{k}). \qquad \text{(B7)}
\end{aligned}$$

The second term (B6):

$$\begin{aligned}
\int d^d\boldsymbol{r} e^{-i\boldsymbol{k}'\cdot\boldsymbol{r}} e^{i\boldsymbol{k}\cdot\boldsymbol{r}} u^*_{\boldsymbol{k}'a'}(\boldsymbol{r}) \frac{\partial}{\partial \boldsymbol{k}} u_{\boldsymbol{k}a}(\boldsymbol{r}) =& \prod_{i=1}^{d} \int_{-\infty}^{\infty} dr_i e^{-i(k'_i - k_i) r_i} u^*_{\boldsymbol{k}'a'}(\boldsymbol{r}) \frac{\partial}{\partial \boldsymbol{k}} u_{\boldsymbol{k}a}(\boldsymbol{r}) \\
=& \prod_{i=1}^{d} \sum_{m_i=-\infty}^{\infty} \int_0^{L_i} dr_i e^{-i(k'_i - k_i)(r_i + m_i L_i)} u^*_{\boldsymbol{k}'a'}(\boldsymbol{r}) \frac{\partial}{\partial \boldsymbol{k}} u_{\boldsymbol{k}a}(\boldsymbol{r}) \\
=& \prod_{i=1}^{d} \sum_{m_i=-\infty}^{\infty} e^{-i(k'_i - k_i) m_i L_i} \int_0^{L_i} dr_i e^{-i(k'_i - k_i) r_i} u^*_{\boldsymbol{k}'a'}(\boldsymbol{r}) \frac{\partial}{\partial \boldsymbol{k}} u_{\boldsymbol{k}a}(\boldsymbol{r}), \qquad \text{(B8)}
\end{aligned}$$

where we divided the integration range by L_i and used periodic condition (B2). We can derive the formula:

$$\sum_{m_i=-\infty}^{\infty} e^{-i(k'_i - k_i) m_i L_i} = \frac{2\pi}{L_i} \delta(k'_i - k_i). \tag{B9}$$

Therefore,

$$\begin{aligned}\int d^d\boldsymbol{r} e^{-i\boldsymbol{k}'\cdot\boldsymbol{r}} e^{i\boldsymbol{k}\cdot\boldsymbol{r}} u^*_{\boldsymbol{k}'a'}(\boldsymbol{r}) \frac{\partial}{\partial\boldsymbol{k}} u_{\boldsymbol{k}a}(\boldsymbol{r}) =& \prod_{i=1}^{d} \frac{2\pi}{L_i}\delta(k'_i - k_i)\int_0^{L_i} dr_i e^{-i(k'_i-k_i)r_i}\ u^*_{\boldsymbol{k}'a'}(\boldsymbol{r})\frac{\partial}{\partial\boldsymbol{k}}u_{\boldsymbol{k}a}(\boldsymbol{r}) \\ =& \frac{(2\pi)^d}{V}\delta(\boldsymbol{k}'-\boldsymbol{k})\int_V d\boldsymbol{r}\ e^{-i(\boldsymbol{k}'-\boldsymbol{k})\cdot\boldsymbol{r}}\ u^*_{\boldsymbol{k}'a'}(\boldsymbol{r})\frac{\partial}{\partial\boldsymbol{k}}u_{\boldsymbol{k}a}(\boldsymbol{r}) \\ =& \frac{(2\pi)^d}{V}\delta(\boldsymbol{k}'-\boldsymbol{k})\int_V d\boldsymbol{r}\ u^*_{\boldsymbol{k}'a'}(\boldsymbol{r})\frac{\partial}{\partial\boldsymbol{k}}u_{\boldsymbol{k}a}(\boldsymbol{r}),\end{aligned} \tag{B10}$$

where V is unit volume $V = \prod_i L_i$. Substituting (B7), (B10) into (B5), (B6),

$$\begin{aligned}\langle\Psi'|\widehat{\boldsymbol{r}}|\Psi\rangle =& \sum_{a',a}\int \frac{d^d\boldsymbol{k}'}{(2\pi)^d}\frac{d^d\boldsymbol{k}}{(2\pi)^d} C^*_{\boldsymbol{k}'a'} i(2\pi)^d\delta_{a'a}\delta(\boldsymbol{k}'-\boldsymbol{k})\left(\frac{\partial}{\partial\boldsymbol{k}}C_{\boldsymbol{k}a}\right) \\ &+\sum_{a',a}\int \frac{d^d\boldsymbol{k}'}{(2\pi)^d}\frac{d^d\boldsymbol{k}}{(2\pi)^d} C^*_{\boldsymbol{k}'a'} i\frac{(2\pi)^d}{V}\delta(\boldsymbol{k}'-\boldsymbol{k})\int_V d\boldsymbol{r}\ u^*_{\boldsymbol{k}'a'}(\boldsymbol{r})\frac{\partial}{\partial\boldsymbol{k}}u_{\boldsymbol{k}a}(\boldsymbol{r})C_{\boldsymbol{k}a} \\ =& \sum_{a',a}\int \frac{d^d\boldsymbol{k}'}{(2\pi)^d}\frac{d^d\boldsymbol{k}}{(2\pi)^d} C^*_{\boldsymbol{k}'a'}\ i(2\pi)^d\delta(\boldsymbol{k}'-\boldsymbol{k})\left(\delta_{a'a}\frac{\partial}{\partial\boldsymbol{k}} - i\boldsymbol{\mathcal{A}}_{a'a}(\boldsymbol{k})\right)C_{\boldsymbol{k}a},\end{aligned} \tag{B11}$$

where we defined Berry connection $\boldsymbol{\mathcal{A}}_{a'a}(\boldsymbol{k})$ as

$$\boldsymbol{\mathcal{A}}_{a'a}(\boldsymbol{k}) = \frac{i}{V}\int_V d\boldsymbol{r}\ u^*_{\boldsymbol{k}'a'}(\boldsymbol{r})\frac{\partial}{\partial\boldsymbol{k}}u_{\boldsymbol{k}a}(\boldsymbol{r}). \tag{B12}$$

When we define the covariant derivative operator:

$$\widehat{\boldsymbol{\mathcal{D}}}_{(\boldsymbol{k}'a')(\boldsymbol{k}a)} \equiv (2\pi)^d\delta(\boldsymbol{k}'-\boldsymbol{k})\left(\delta_{a'a}\frac{\partial}{\partial\boldsymbol{k}} - i\boldsymbol{\mathcal{A}}_{a'a}(\boldsymbol{k})\right), \tag{B13}$$

by comparing the above two, we get the relation between $\widehat{\boldsymbol{r}}$ and $\widehat{\boldsymbol{\mathcal{D}}}$:

$$\widehat{\boldsymbol{r}} = i\widehat{\boldsymbol{\mathcal{D}}}. \tag{B14}$$

Similarly, we can calculate evaluate the matrix element of general operator $\widehat{\mathcal{O}}$:

$$\langle\psi_{\boldsymbol{k}'a'}|\widehat{\mathcal{O}}|\psi_{\boldsymbol{k}a}\rangle = (2\pi)^d\delta(\boldsymbol{k}'-\boldsymbol{k})\langle u_{\boldsymbol{k}'a'}|\widehat{\mathcal{O}}(\boldsymbol{k})|u_{\boldsymbol{k}a}\rangle_V \tag{B15}$$

$$\langle u_{\boldsymbol{k}'a'}|\widehat{\mathcal{O}}(\boldsymbol{k})|u_{\boldsymbol{k}a}\rangle_V = \frac{1}{V}\int_V d\boldsymbol{r}\ u^*_{\boldsymbol{k}'a'}(\boldsymbol{r})\langle\boldsymbol{r}|\widehat{\mathcal{O}}(\boldsymbol{k})|u_{\boldsymbol{k}a}\rangle, \tag{B16}$$

where $\widehat{\mathcal{O}}(\boldsymbol{k}) \equiv e^{-i\boldsymbol{k}\cdot\widehat{\boldsymbol{r}}}\widehat{\mathcal{O}}e^{i\boldsymbol{k}\cdot\widehat{\boldsymbol{r}}}$ is the k-dependent operator.

3. Electromagnetic interactions

Electromagnetic perturbation is realized by gauge principle replacing $\boldsymbol{k} \to \boldsymbol{k} - q\boldsymbol{A}(t)$ where the vector potential $A(t)$ is chosen so that $\boldsymbol{E}(t) = -\partial_t\boldsymbol{A}(t)$.

$$\widehat{H}_A(\boldsymbol{k},t) = \widehat{H}_0\left(\boldsymbol{k} - q\boldsymbol{A}(t)\right). \tag{B17}$$

Using (B3), (B14) and BCH formula:

$$e^{\widehat{A}}\widehat{B}e^{-\widehat{A}} = \widehat{B} + \left[\widehat{A},\widehat{B}\right] + \frac{1}{2}\left[\widehat{A},\left[\widehat{A},\widehat{B}\right]\right] + \cdots, \tag{B18}$$

the Hamiltonian becomes,

$$\begin{aligned}\widehat{H}_A(\boldsymbol{k},t) &= e^{-i(\boldsymbol{k}-q\boldsymbol{A})\cdot\widehat{\boldsymbol{r}}}\ \widehat{H}_0\ e^{i(\boldsymbol{k}-q\boldsymbol{A})\cdot\widehat{\boldsymbol{r}}} \\ &= e^{q\boldsymbol{A}\cdot\widehat{\boldsymbol{\mathcal{D}}}}\ \widehat{H}_0(\boldsymbol{k})\ e^{-q\boldsymbol{A}\cdot\widehat{\boldsymbol{\mathcal{D}}}} \\ &= \widehat{H}_0(\boldsymbol{k}) + \left[q\boldsymbol{A}\cdot\widehat{\boldsymbol{\mathcal{D}}}, \widehat{H}_0(\boldsymbol{k})\right] + \frac{1}{2}\left[q\boldsymbol{A}\cdot\widehat{\boldsymbol{\mathcal{D}}}, \left[q\boldsymbol{A}\cdot\widehat{\boldsymbol{\mathcal{D}}}, \widehat{H}_0(\boldsymbol{k})\right]\right] + \cdots \\ &= \widehat{H}_0(\boldsymbol{k}) + \sum_{n=1}^{\infty}\frac{1}{n!}\left[\prod_{k=1}^{n} qA^{\alpha_k}\widehat{\mathcal{D}}^{\alpha_k}\right]\widehat{H}_0(\boldsymbol{k}) \\ &= \widehat{H}_0(\boldsymbol{k}) + \sum_{n=1}^{\infty}\frac{1}{n!}\prod_{k=1}^{n} qA^{\alpha_k}\widehat{h}^{\alpha_1\cdots\alpha_n}(\boldsymbol{k}),\end{aligned} \tag{B19}$$

where α_k is a spacial index with an implicit sum. Note that we use the following shorthands:

$$\widehat{\boldsymbol{\mathcal{D}}}[\widehat{\mathcal{O}}] \equiv [\widehat{\boldsymbol{\mathcal{D}}},\ \widehat{\mathcal{O}}] \tag{B20}$$

$$\widehat{h}^{\alpha_1\cdots\alpha_n} \equiv \widehat{\mathcal{D}}^{\alpha_1}\cdots\widehat{\mathcal{D}}^{\alpha_n}[\widehat{H}_0]. \tag{B21}$$

Finally, we go back to the k-independent form [2] ,

$$\begin{aligned}\widehat{H}_A(t) &\equiv e^{i\boldsymbol{k}\cdot\widehat{\boldsymbol{r}}}\widehat{H}_A(\boldsymbol{k},t)e^{-i\boldsymbol{k}\cdot\widehat{\boldsymbol{r}}} \\ &= \widehat{H}_0 + \sum_{n=1}^{\infty}\frac{1}{n!}\prod_{k=1}^{n} qA^{\alpha_k}\widehat{h}^{\alpha_1\cdots\alpha_n}.\end{aligned} \tag{B22}$$

The second term of (B22) represents the perturbation due to the external field ($\equiv V_E(t)$).

We perform the Fourier transformation:

$$\boldsymbol{A}(t) = \int d\omega e^{-i(\omega+i\gamma)t}\boldsymbol{A}(\omega) \tag{B23}$$

$$\boldsymbol{E}(\omega) = i\omega\boldsymbol{A}(\omega), \tag{B24}$$

where γ is a small and positive real number describing electron scattering. It satisfies the assumption that the initial state is in equilibrium $A(t)|_{t\to-\infty} = 0$. To avoid notational complexity, we omit γ in the following calculations and reintroduce it later. The perturbation becomes,

$$\begin{aligned}V_E(t) &= \sum_{m=1}^{\infty}\frac{1}{m!}\prod_{j=1}^{m}\int d\omega_j e^{-i\omega_j t}\left(\frac{-iq}{\omega_j}\right)E^{\alpha_j}(\omega_j)\widehat{h}^{\alpha_1\cdots\alpha_m} \\ &= \sum_{m=1}^{\infty}\frac{1}{m!}\prod_{j=1}^{m}\int d\omega_j e^{-i\omega_j t}\left(\frac{ie}{\omega_j}\right)E^{\alpha_j}(\omega_j)\widehat{h}^{\alpha_1\cdots\alpha_m},\end{aligned} \tag{B25}$$

where $q = -e,\ (e > 0)$ for electron case. Using (B15), $\widehat{h}$ can be expanded by its matrix elements $h_{\boldsymbol{k}aa'} \equiv \langle\psi_{\boldsymbol{k}a}|\widehat{h}|\psi_{\boldsymbol{k}a'}\rangle$ which means:

$$\widehat{h}^{\alpha_1\cdots\alpha_n} = \sum_{aa'}\int\frac{d^d\boldsymbol{k}}{(2\pi)^d}c^\dagger_{\boldsymbol{k}a}h^{\alpha_1\ldots\alpha_n}_{\boldsymbol{k}aa'}c_{\boldsymbol{k}a'}. \tag{B26}$$

[2] $\widehat{\boldsymbol{\mathcal{D}}}$ and $e^{\pm i\boldsymbol{k}\cdot\widehat{\boldsymbol{r}}}$ are commutable since $\widehat{\boldsymbol{r}} = i\widehat{\boldsymbol{\mathcal{D}}}$. Therefore, we can use $\widehat{\boldsymbol{\mathcal{D}}} = e^{i\boldsymbol{k}\cdot\widehat{\boldsymbol{r}}}\widehat{\boldsymbol{\mathcal{D}}}e^{-i\boldsymbol{k}\cdot\widehat{\boldsymbol{r}}}$ to derive (B22).

Appendix C: General calculation of the optical response

In this section, we calculate the optical response up to the second order.

1. Partition function

Consider the path-integral form of partition function:

$$Z = \int_{\xi_f=-\xi_i} \mathcal{D}\xi^* \mathcal{D}\xi \, e^{-S} \tag{C1}$$

$$S = \int_0^\beta d\tau \sum_{aa'} \int \frac{d^d\boldsymbol{k}}{(2\pi)^d} \left[\delta_{aa'} \xi^*_{\boldsymbol{k}a}(\tau) \frac{\partial \xi_{\boldsymbol{k}a'}(\tau)}{\partial \tau} + H_0(\xi^*_{\boldsymbol{k}a}(\tau), \xi_{\boldsymbol{k}a'}(\tau)) + V_E(\xi^*_{\boldsymbol{k}a}(\tau), \xi_{\boldsymbol{k}a'}(\tau)) \right] \tag{C2}$$

$$H_0(\xi^*_{\boldsymbol{k}a}(\tau), \xi_{\boldsymbol{k}a'}(\tau)) = \delta_{aa'} \xi^*_{\boldsymbol{k}a'}(\tau) \varepsilon_{\boldsymbol{k}a'} \xi_{\boldsymbol{k}a'}(\tau) \tag{C3}$$

$$V_E(\xi^*_{\boldsymbol{k}a}(\tau), \xi_{\boldsymbol{k}a'}(\tau)) = \sum_{m=1}^{\infty} \frac{1}{m!} \prod_{j=1}^{m} i \int d\omega_{n;j} e^{-i\omega_{n;j}\tau} \left(\frac{e}{\omega_{n;j}} \right) E^{\alpha_j}(\omega_{n;j}) \xi^*_{\boldsymbol{k}a}(\tau) h^{\alpha_1\ldots\alpha_m}_{\boldsymbol{k}aa'} \xi_{\boldsymbol{k}a'}(\tau), \tag{C4}$$

where[3]

$$\tau = it, \quad \omega_{n;j} = -i\omega_j, \quad E^{\alpha_j}(\omega_{n;j}) \equiv E^{\alpha_j}(\omega_j), \quad V_E(\tau) \equiv V_E(t). \tag{C5}$$

We perform Fourier transformation [4] :

$$\xi_{\boldsymbol{k}a}(\tau) = \frac{1}{\beta} \sum_n \xi_{\boldsymbol{k}a}(\omega_n) e^{-i\omega_n\tau}, \quad \xi^*_{\boldsymbol{k}a}(\tau) = \frac{1}{\beta} \sum_n \xi^*_{\boldsymbol{k}a}(\omega_n) e^{i\omega_n\tau}, \tag{C6}$$

where ω_n is called Matsubara frequency ($\omega_n = (2n+1)\pi/\beta$)[5]. Then, the non-perturbative action S_0 becomes,

$$\begin{aligned} S_0 &= \int_0^\beta d\tau \sum_a \int \frac{d^d\boldsymbol{k}}{(2\pi)^d} \left[\xi^*_{\boldsymbol{k}a}(\tau) \frac{\partial \xi_{\boldsymbol{k}a}(\tau)}{\partial \tau} + \xi^*_{\boldsymbol{k}a}(\tau) \varepsilon_{\boldsymbol{k}a} \xi_{\boldsymbol{k}a}(\tau) \right] \\ &= \int_0^\beta d\tau \sum_a \int \frac{d^d\boldsymbol{k}}{(2\pi)^d} \frac{1}{\beta^2} \sum_{n,n'} e^{i(\omega_n-\omega_{n'})\tau} \left[-\xi^*_{\boldsymbol{k}a}(\omega_n) i\omega_{n'} \xi_{\boldsymbol{k}a}(\omega_{n'}) + \xi^*_{\boldsymbol{k}a}(\omega_n) \varepsilon_{\boldsymbol{k}a} \xi_{\boldsymbol{k}a}(\omega_{n'}) \right]. \end{aligned} \tag{C7}$$

We can calculate τ integration with

$$\int_0^\beta d\tau e^{i(\omega_n-\omega_{n'})\tau} = \beta \delta_{nn'}. \tag{C8}$$

The Fourier transformed action is

$$\begin{aligned} S_0 &= \sum_a \int \frac{d^d\boldsymbol{k}}{(2\pi)^d} \frac{1}{\beta^2} \sum_{n,n'} \beta \delta_{nn'} \left[-\xi^*_{\boldsymbol{k}a}(\omega_n) i\omega_{n'} \xi_{\boldsymbol{k}a}(\omega_{n'}) + \xi^*_{\boldsymbol{k}a}(\omega_n) \varepsilon_{\boldsymbol{k}a} \xi_{\boldsymbol{k}a}(\omega_{n'}) \right] \\ &= \sum_a \int \frac{d^d\boldsymbol{k}}{(2\pi)^d} \frac{1}{\beta} \sum_n \left[-\xi^*_{\boldsymbol{k}a}(\omega_n) i\omega_n \xi_{\boldsymbol{k}a}(\omega_n) + \xi^*_{\boldsymbol{k}a}(\omega_n) \varepsilon_{\boldsymbol{k}a} \xi_{\boldsymbol{k}a}(\omega_n) \right], \end{aligned} \tag{C9}$$

---

[3] Since $\omega_{n;j}$ is discrete, $\int d\omega_{n;j}$ actually means $\sum_{\omega_{n;j}}$. For the convenience, we keep to white it as $\int d\omega_{n;j}$.

[4] The inverse transformation is: $\xi_{\boldsymbol{k}a}(\omega_n) = \int_0^\beta d\tau \xi_{\boldsymbol{k}a}(\tau) e^{i\omega_n\tau}$, $\xi^*_{\boldsymbol{k}a}(\omega_n) = \int_0^\beta d\tau \xi^*_{\boldsymbol{k}a}(\tau) e^{-i\omega_n\tau}$.

[5] This discreteness is from the boundary condition $\xi_f = -\xi_i$.

and the non-perturbative partition function Z_0 becomes,

$$
\begin{aligned}
Z_0 =&|J| \int \mathcal{D}\xi^* \mathcal{D}\xi \prod_{n,\boldsymbol{k},a} e^{-\xi^*_{\boldsymbol{k}a}(\omega_n)(-i\omega_n+\varepsilon_{\boldsymbol{k}a})\xi_{\boldsymbol{k}a}(\omega_n)} \\
=&|J| \prod_{n,\boldsymbol{k},a} (-1)\frac{1}{\beta}(i\omega_n - \varepsilon_{\boldsymbol{k}a}),
\end{aligned} \tag{C10}
$$

where $|J|$ is Jacobian for (C6) and we used Gaussian integral for Grassmann variables:

$$
\int d\xi^* d\xi \, e^{-\xi^* M \xi} = \det M. \tag{C11}
$$

2. Green function

We introduce Green function

$$
G_{\boldsymbol{k}aa'}(\tau,\tau') \equiv -\langle \mathrm{T} c_{\boldsymbol{k}a}(\tau) c^\dagger_{\boldsymbol{k}a'}(\tau')\rangle = -\mathrm{Tr}\left(e^{-\beta\widehat{H}} c_{\boldsymbol{k}a}(\tau) c^\dagger_{\boldsymbol{k}a'}(\tau')\right). \tag{C12}
$$

Applying Heisenberg picture $c_{\boldsymbol{k}a}(\tau) = e^{\tau\widehat{H}} c_{\boldsymbol{k}a}(0) e^{-\tau\widehat{H}}$, $\;c^\dagger_{\boldsymbol{k}a}(\tau) = e^{\tau\widehat{H}} c^\dagger_{\boldsymbol{k}a}(0) e^{-\tau\widehat{H}}$,

$$
\begin{aligned}
G_{\boldsymbol{k}aa'}(\tau,\tau') =& - \mathrm{Tr}\left(e^{-\beta\widehat{H}} e^{\tau\widehat{H}} c_{\boldsymbol{k}a}(0) e^{-\tau\widehat{H}} e^{\tau'\widehat{H}} c^\dagger_{\boldsymbol{k}a'}(0) e^{-\tau'\widehat{H}}\right) \\
=& - \mathrm{Tr}\left(e^{-\beta\widehat{H}} e^{(\tau-\tau')\widehat{H}} c_{\boldsymbol{k}a}(0) e^{-(\tau-\tau')\widehat{H}} c^\dagger_{\boldsymbol{k}a'}(0)\right) \\
=& G_{\boldsymbol{k}aa'}(\tau-\tau',0),
\end{aligned} \tag{C13}
$$

where we used trace technique $\mathrm{Tr}(ABC) = \mathrm{Tr}(CAB)$. Therefore, the Green function depends only on $\tau-\tau'$ and we can replace $\tau-\tau'$ to τ without generality. Here is the new convention:

$$
G_{\boldsymbol{k}aa'}(\tau) \equiv -\langle \mathrm{T} c_{\boldsymbol{k}a}(\tau) c^\dagger_{\boldsymbol{k}a'}(0)\rangle. \tag{C14}
$$

The path integral form for each convention is,

$$
G_{\boldsymbol{k}aa'}(\tau,\tau') = -\frac{1}{Z_0}\int \mathcal{D}\xi^*\mathcal{D}\xi \, \xi_{\boldsymbol{k}a}(\tau)\xi^*_{\boldsymbol{k}a'}(\tau') e^{-S_0} \tag{C15}
$$

$$
G_{\boldsymbol{k}aa'}(\tau) = -\frac{1}{Z_0}\int \mathcal{D}\xi^*\mathcal{D}\xi \, \xi_{\boldsymbol{k}a}(\tau)\xi^*_{\boldsymbol{k}a'}(0) e^{-S_0}. \tag{C16}
$$

Let us derive its Fourier transformation. Applying (C6),

$$
G_{\boldsymbol{k}aa'}(\tau) = -\frac{1}{Z_0}|J| \int \mathcal{D}\xi^*\mathcal{D}\xi \, \frac{1}{\beta^2}\sum_{n,n'} \xi_{\boldsymbol{k}a}(\omega_n) e^{-i\omega_n\tau} \xi^*_{\boldsymbol{k}a'}(\omega_{n'}) e^{-S_0}. \tag{C17}
$$

This Grassmann integral has non-zero value only for $(n,a) = (n',a')$. Thus,

$$
\begin{aligned}
G_{\boldsymbol{k}aa'}(\tau) =& -\frac{1}{Z_0}|J| \int \mathcal{D}\xi^*\mathcal{D}\xi \, \frac{1}{\beta^2}\sum_{n,n'} \delta_{nn'}\delta_{aa'} \xi_{\boldsymbol{k}a}(\omega_n) e^{-i\omega_n\tau} \xi^*_{\boldsymbol{k}a'}(\omega_{n'}) e^{-S_0} \\
=& \frac{1}{\beta}\sum_n \left(-\frac{1}{Z_0}|J|\delta_{aa'}\int \mathcal{D}\xi^*\mathcal{D}\xi \, \frac{1}{\beta}\xi_{\boldsymbol{k}a}(\omega_n)\xi^*_{\boldsymbol{k}a'}(\omega_n) e^{-S_0}\right) e^{-i\omega_n\tau}.
\end{aligned} \tag{C18}
$$

Then we can define and calculate the Fourier transformation,

$$
\begin{aligned}
G_{\boldsymbol{k}aa'}(\omega_n) \equiv& -\frac{1}{Z_0}|J|\delta_{aa'}\int \mathcal{D}\xi^*\mathcal{D}\xi \, \frac{1}{\beta}\xi_{\boldsymbol{k}a}(\omega_n)\xi^*_{\boldsymbol{k}a'}(\omega_n) e^{-S_0} \\
=& -\delta_{aa'}\frac{1}{\beta}\frac{|J|\prod_{(m,\boldsymbol{k}',a'')\neq(n,\boldsymbol{k},a)}(-1)(1/\beta)(i\omega_m - \varepsilon_{\boldsymbol{k}'a''})}{|J|\prod_{(m,\boldsymbol{k}',a'')}(-1)(1/\beta)(i\omega_m - \varepsilon_{\boldsymbol{k}'a''})} \\
=& \delta_{aa'}\frac{1}{i\omega_n - \varepsilon_{\boldsymbol{k}a}},
\end{aligned} \tag{C19}
$$

where we used the formula:

$$\int d\xi^* d\xi\, \xi\xi^* e^{-\xi^* M\xi} = \int d\xi^* d\xi\, \xi\xi^*(1-\xi^* M\xi) = 1. \tag{C20}$$

Substituting (C19) into (C18) , we obtain the inverse Fourier transformation:

$$G_{\boldsymbol{k}aa'}(\tau) = \frac{1}{\beta}\sum_n \left(\delta_{aa'}\frac{1}{i\omega_n - \varepsilon_{\boldsymbol{k}a}}\right) e^{-i\omega_n\tau} = \delta_{aa'}\frac{1}{\beta}\sum_n \frac{e^{-i\omega_n\tau}}{i\omega_n - \varepsilon_{\boldsymbol{k}a}}. \tag{C21}$$

3. Source fields

We introduce source fields $\{\overline{\alpha}_{\boldsymbol{k}a}(\tau),\ \gamma_{\boldsymbol{k}a}(\tau)\}$ for $\{\xi_{\boldsymbol{k}a}(\tau),\ \xi^*_{\boldsymbol{k}a}(\tau)\}$. Then, the non-perturbative action $S_{0,\overline{\alpha},\gamma}$ is,

$$S_{0,\overline{\alpha},\gamma} = \int_0^\beta d\tau \sum_a \int \frac{d^d\boldsymbol{k}}{(2\pi)^d}\left[\xi^*_{\boldsymbol{k}a}(\tau)\frac{\partial\xi_{\boldsymbol{k}a}(\tau)}{\partial\tau} + \xi^*_{\boldsymbol{k}a}(\tau)\varepsilon_{\boldsymbol{k}a}\xi_{\boldsymbol{k}a}(\tau) + \overline{\alpha}_{\boldsymbol{k}a}(\tau)\xi_{\boldsymbol{k}a}(\tau) + \xi^*_{\boldsymbol{k}a}(\tau)\gamma_{\boldsymbol{k}a}(\tau)\right]. \tag{C22}$$

We perform Fourier transformation:

$$\gamma_{\boldsymbol{k}}(\tau) = \frac{1}{\beta}\sum_n \gamma_{\boldsymbol{k}}(\omega_n)e^{-i\omega_n\tau}, \quad \overline{\alpha}_{\boldsymbol{k}}(\tau) = \frac{1}{\beta}\sum_n \overline{\alpha}_{\boldsymbol{k}}(\omega_n)e^{i\omega_n\tau}. \tag{C23}$$

The action becomes,

$$S_{0,\overline{\alpha},\gamma} = \sum_a \int \frac{d^d\boldsymbol{k}}{(2\pi)^d}\frac{1}{\beta}\sum_n \left[\xi^*_{\boldsymbol{k}a}(\omega_n)(-i\omega_n+\varepsilon_{\boldsymbol{k}a})\xi_{\boldsymbol{k}a}(\omega_n) + \overline{\alpha}_{\boldsymbol{k}a}(\omega_n)\xi_{\boldsymbol{k}a}(\omega_n) + \xi^*_{\boldsymbol{k}a}(\omega_n)\gamma_{\boldsymbol{k}a}(\omega_n)\right]. \tag{C24}$$

We calculate the inside part,

$$\begin{aligned}
&\xi^*_{\boldsymbol{k}a}(\omega_n)(-i\omega_n+\varepsilon_{\boldsymbol{k}a})\xi_{\boldsymbol{k}a}(\omega_n) + \overline{\alpha}_{\boldsymbol{k}a}(\omega_n)\xi_{\boldsymbol{k}a}(\omega_n) + \xi^*_{\boldsymbol{k}a}(\omega_n)\gamma_{\boldsymbol{k}a}(\omega_n)\\
=&(-i\omega_n+\varepsilon_{\boldsymbol{k}a})\left[\xi^*_{\boldsymbol{k}a}(\omega_n)\xi_{\boldsymbol{k}a}(\omega_n) + \frac{\overline{\alpha}_{\boldsymbol{k}a}(\omega_n)}{-i\omega_n+\varepsilon_{\boldsymbol{k}a}}\xi_{\boldsymbol{k}a}(\omega_n) + \xi^*_{\boldsymbol{k}a}(\omega_n)\frac{\gamma_{\boldsymbol{k}a}(\omega_n)}{-i\omega_n+\varepsilon_{\boldsymbol{k}a}}\right]\\
=&(-i\omega_n+\varepsilon_{\boldsymbol{k}a})\left[\left(\xi^*_{\boldsymbol{k}a}(\omega_n) + \frac{\overline{\alpha}_{\boldsymbol{k}a}(\omega_n)}{-i\omega_n+\varepsilon_{\boldsymbol{k}a}}\right)\left(\xi_{\boldsymbol{k}a}(\omega_n) + \frac{\gamma_{\boldsymbol{k}a}(\omega_n)}{-i\omega_n+\varepsilon_{\boldsymbol{k}a}}\right) - \frac{\overline{\alpha}_{\boldsymbol{k}a}(\omega_n)}{-i\omega_n+\varepsilon_{\boldsymbol{k}a}}\frac{\gamma_{\boldsymbol{k}a}(\omega_n)}{-i\omega_n+\varepsilon_{\boldsymbol{k}a}}\right].
\end{aligned} \tag{C25}$$

We shift the fields:

$$\chi^*_{\boldsymbol{k}a}(\omega_n) = \xi^*_{\boldsymbol{k}a}(\omega_n) + \frac{\overline{\alpha}_{\boldsymbol{k}a}(\omega_n)}{-i\omega_n+\varepsilon_{\boldsymbol{k}a}}, \quad \chi_{\boldsymbol{k}a}(\omega_n) = \xi_{\boldsymbol{k}a}(\omega_n) + \frac{\gamma_{\boldsymbol{k}a}(\omega_n)}{-i\omega_n+\varepsilon_{\boldsymbol{k}a}}. \tag{C26}$$

Then,

$$\begin{aligned}
Z_{0,\overline{\alpha},\gamma} =& \int \mathcal{D}\chi^*\mathcal{D}\chi \exp\left[\sum_a \int \frac{d^d\boldsymbol{k}}{(2\pi)^d}\frac{1}{\beta}\sum_n -\chi^*_{\boldsymbol{k}a}(\omega_n)(-i\omega_n+\varepsilon_{\boldsymbol{k}a})\chi_{\boldsymbol{k}a}(\omega_n) + \frac{\overline{\alpha}_{\boldsymbol{k}a}(\omega_n)\gamma_{\boldsymbol{k}a}(\omega_n)}{-i\omega_n+\varepsilon_{\boldsymbol{k}a}}\right]\\
=&Z_0 \exp\left[\sum_a \int \frac{d^d\boldsymbol{k}}{(2\pi)^d}\frac{1}{\beta}\sum_n \overline{\alpha}_{\boldsymbol{k}a}(\omega_n)\frac{1}{-i\omega_n+\varepsilon_{\boldsymbol{k}a}}\gamma_{\boldsymbol{k}a}(\omega_n)\right]\\
=&Z_0 \exp\left[\sum_{aa'} \int \frac{d^d\boldsymbol{k}}{(2\pi)^d} d\tau d\tau' \overline{\alpha}_{\boldsymbol{k}a}(\tau)\left(-G_{\boldsymbol{k}aa'}(\tau-\tau')\right)\gamma_{\boldsymbol{k}a'}(\tau')\right].
\end{aligned} \tag{C27}$$

We can derive that[6]

$$G_{\boldsymbol{k}aa'}(\tau-\tau') = \frac{1}{Z_0}\frac{\delta}{\delta\overline{\alpha}_{\boldsymbol{k}a}(\tau)}\frac{\delta}{\delta\gamma_{\boldsymbol{k}a'}(\tau')}Z_{0,\overline{\alpha},\gamma}\Big|_{\overline{\alpha}=\gamma=0}. \tag{C28}$$

---

[6] The munus sign in (C27) is canceled by the anti-commutation of $\delta\gamma$ and $\overline{\alpha}$ in the first derivative.

We have the formula:

$$\frac{\delta}{\delta\overline{\alpha}_{\boldsymbol{k}a}(\tau)} Z_{0,\overline{\alpha},\gamma}\bigg|_{\overline{\alpha}=\gamma=0} = \int \mathcal{D}\xi^* \mathcal{D}\xi \, \xi_{\boldsymbol{k}a}(\tau) e^{-S_0} \tag{C29}$$

$$\frac{-\delta}{\delta\gamma_{\boldsymbol{k}a'}(\tau')} Z_{0,\overline{\alpha},\gamma}\bigg|_{\overline{\alpha}=\gamma=0} = \int \mathcal{D}\xi^* \mathcal{D}\xi \, \xi^*_{\boldsymbol{k}a'}(\tau') e^{-S_0}. \tag{C30}$$

Therefore, with the interaction,

$$\begin{aligned}
Z =& \exp\left[-\int_0^\beta d\tau \sum_{aa'} \int \frac{d^d\boldsymbol{k}}{(2\pi)^d} V_E\left(\frac{\delta}{\delta\overline{\alpha}_{\boldsymbol{k}a}(\tau)}, \frac{-\delta}{\delta\gamma_{\boldsymbol{k}a'}(\tau)}\right)\right] Z_{0,\overline{\alpha},\gamma}\bigg|_{\overline{\alpha}=\gamma=0} \\
=& \exp\Bigg[-\int_0^\beta d\tau \sum_{aa'} \int \frac{d^d\boldsymbol{k}}{(2\pi)^d} \sum_{m=1}^\infty \frac{1}{m!} \prod_{j=1}^m i \int d\omega_{n;j} e^{-i\omega_{n;j}\tau} \\
&\times \left(\frac{e}{\omega_{n;j}}\right) E^{\alpha_k}(\omega_{n;j}) \frac{-\delta}{\delta\gamma_{\boldsymbol{k}a}(\tau)} h^{\alpha_1\ldots\alpha_m}_{\boldsymbol{k}aa'} \frac{\delta}{\delta\overline{\alpha}_{\boldsymbol{k}a'}(\tau)}\Bigg] Z_{0,\overline{\alpha},\gamma}\big|_{\overline{\alpha}=\gamma=0}.
\end{aligned} \tag{C31}$$

4. The expectation value of the current

The expectation value of the output current is,

$$\langle \widehat{J}^\mu \rangle(\tau) = \frac{1}{Z} \int \mathcal{D}\xi^* \mathcal{D}\xi \, \left[e v^\mu_E(\tau) e^{-S} \right], \tag{C32}$$

where $\widehat{v}^\mu_E(\tau)$ is the velocity operator obtained by the analytic continuation $\widehat{v}^\mu_E(\tau) \equiv \widehat{v}^\mu_E(t)$, with $\widehat{v}^\mu_E(t) \equiv \dot{\widehat{r}}^\mu = -i[\widehat{r}^\mu, \, \widehat{H}_0 + \widehat{V}_E(t)]$ governed by Heisenberg equation of motion:

$$\begin{aligned}
\widehat{v}^\mu_E(\tau) \equiv& \widehat{\mathcal{D}}^\mu[\widehat{H}_0 + \widehat{V}_E(\tau)] \\
=& \widehat{h}^\mu + \sum_{m=1}^\infty \frac{1}{m!} \prod_{j=1}^m i \int d\omega_{n;j} e^{-i\omega_{n;j}\tau} \left(\frac{e}{\omega_{n;j}}\right) E^{\alpha_j}(\omega_{n;j}) \widehat{h}^{\mu\alpha_1\ldots\alpha_m} \\
=& \sum_{aa'} \int \frac{d^d\boldsymbol{k}}{(2\pi)^d} \left\{ c^\dagger_{\boldsymbol{k}a} h^\mu_{\boldsymbol{k}aa'} c_{\boldsymbol{k}a'} + \sum_{m=1}^\infty \frac{1}{m!} \prod_{j=1}^m i \int d\omega_{n;j} e^{-i\omega_{n;j}\tau} \left(\frac{e}{\omega_{n;j}}\right) E^{\alpha_j}(\omega_{n;j}) c^\dagger_{\boldsymbol{k}a} h^{\mu\alpha_1\ldots\alpha_m}_{\boldsymbol{k}aa'} c_{\boldsymbol{k}a'} \right\}.
\end{aligned} \tag{C33}$$

Thus,

$$\begin{aligned}
\langle \widehat{J}^\mu \rangle(\tau) =& \frac{e}{Z} \Bigg[\sum_{aa'} \int \frac{d^d\boldsymbol{k}}{(2\pi)^d} \Bigg\{ \frac{-\delta}{\delta\gamma_{\boldsymbol{k}a}(\tau)} h^\mu_{\boldsymbol{k}aa'} \frac{\delta}{\delta\overline{\alpha}_{\boldsymbol{k}a'}(\tau)} \\
&+ \sum_{m=1}^\infty \frac{1}{m!} \prod_{j=1}^m i \int d\omega_{n;j} e^{-i\omega_{n;j}\tau} \left(\frac{e}{\omega_{n;j}}\right) E^{\alpha_j}(\omega_{n;j}) \frac{-\delta}{\delta\gamma_{\boldsymbol{k}a}(\tau)} h^{\mu\alpha_1\ldots\alpha_m}_{\boldsymbol{k}aa'} \frac{\delta}{\delta\overline{\alpha}_{\boldsymbol{k}a'}(\tau)} \Bigg\} \Bigg] \\
&\times \exp\Bigg[-\int_0^\beta d\tau \sum_{aa'} \int \frac{d^d\boldsymbol{k}}{(2\pi)^d} \sum_{m=1}^\infty \frac{1}{m!} \prod_{j=1}^m i \int d\omega_{n;j} e^{-i\omega_{n;j}\tau} \\
&\times \left(\frac{e}{\omega_{n;j}}\right) E^{\alpha_k}(\omega_{n;j}) \frac{-\delta}{\delta\gamma_{\boldsymbol{k}a}(\tau)} h^{\alpha_1\ldots\alpha_m}_{\boldsymbol{k}aa'} \frac{\delta}{\delta\overline{\alpha}_{\boldsymbol{k}a'}(\tau)}\Bigg] Z_{0,\overline{\alpha},\gamma}\big|_{\overline{\alpha}=\gamma=0}.
\end{aligned} \tag{C34}$$

The first $[\cdots]$ part can be expanded as below:

$$
\begin{aligned}
&\sum_{aa'}\int\frac{d^d\boldsymbol{k}}{(2\pi)^d}\left\{\frac{-\delta}{\delta\gamma_{\boldsymbol{k}a}(\tau)}h^{\mu}_{\boldsymbol{k}aa'}\frac{\delta}{\delta\overline{\alpha}_{\boldsymbol{k}a'}(\tau)}\right.\\
&\qquad\left.+\sum_{m=1}^{\infty}\frac{1}{m!}\prod_{j=1}^{m}i\int d\omega_{n;j}e^{-i\omega_{n;j}\tau}\left(\frac{e}{\omega_{n;j}}\right)E^{\alpha_j}(\omega_{n;j})\frac{-\delta}{\delta\gamma_{\boldsymbol{k}a}(\tau)}h^{\mu\alpha_1\ldots\alpha_m}_{\boldsymbol{k}aa'}\frac{\delta}{\delta\overline{\alpha}_{\boldsymbol{k}a'}(\tau)}\right\}\\
=&\sum_{aa'}\int\frac{d^d\boldsymbol{k}}{(2\pi)^d}\left\{\frac{-\delta}{\delta\gamma_{\boldsymbol{k}a}(\tau)}h^{\mu}_{\boldsymbol{k}aa'}\frac{\delta}{\delta\overline{\alpha}_{\boldsymbol{k}a'}(\tau)}\right.\\
&\qquad+i\int d\omega_{n;1}e^{-i\omega_{n;1}\tau}\left(\frac{e}{\omega_{n;1}}\right)E^{\alpha_1}(\omega_{n;1})\frac{-\delta}{\delta\gamma_{\boldsymbol{k}a}(\tau)}h^{\mu\alpha_1}_{\boldsymbol{k}aa'}\frac{\delta}{\delta\overline{\alpha}_{\boldsymbol{k}a'}(\tau)}\\
&\qquad\left.+\frac{1}{2!}i^2\int d\omega_{n;1}d\omega_{n;2}e^{-i(\omega_{n;1}+\omega_{n;2})\tau}\left(\frac{e^2}{\omega_{n;1}\omega_{n;2}}\right)E^{\alpha_1}(\omega_{n;1})E^{\alpha_2}(\omega_{n;2})\frac{-\delta}{\delta\gamma_{\boldsymbol{k}a}(\tau)}h^{\mu\alpha_1\alpha_2}_{\boldsymbol{k}aa'}\frac{\delta}{\delta\overline{\alpha}_{\boldsymbol{k}a'}(\tau)}\right\}\\
&\qquad+\mathcal{O}(E^3).
\end{aligned}
\tag{C35}
$$

The exponential part can be expanded as below:

$$
\begin{aligned}
&\exp\left[-\int_0^{\beta}d\tau\sum_{aa'}\int\frac{d^d\boldsymbol{k}}{(2\pi)^d}\sum_{m=1}^{\infty}\frac{1}{m!}\prod_{j=1}^{m}i\int d\omega_{n;j}e^{-i\omega_{n;j}\tau}\left(\frac{e}{\omega_{n;j}}\right)E^{\alpha_k}(\omega_{n;j})\frac{-\delta}{\delta\gamma_{\boldsymbol{k}a}(\tau)}h^{\alpha_1\ldots\alpha_m}_{\boldsymbol{k}aa'}\frac{\delta}{\delta\overline{\alpha}_{\boldsymbol{k}a'}(\tau)}\right]\\
=&\exp\left[-\int_0^{\beta}d\tau\sum_{aa'}\int\frac{d^d\boldsymbol{k}}{(2\pi)^d}\left\{i\int d\omega_{n;1}e^{-i\omega_{n;1}\tau}\left(\frac{e}{\omega_{n;1}}\right)E^{\alpha_1}(\omega_{n;1})\frac{-\delta}{\delta\gamma_{\boldsymbol{k}a}(\tau)}h^{\alpha_1}_{\boldsymbol{k}aa'}\frac{\delta}{\delta\overline{\alpha}_{\boldsymbol{k}a'}(\tau)}\right.\right.\\
&\quad\left.\left.+\frac{1}{2!}i^2\int d\omega_{n;1}d\omega_{n;2}e^{-i(\omega_{n;1}+\omega_{n;2})\tau}\left(\frac{e^2}{\omega_{n;1}\omega_{n;2}}\right)E^{\alpha_k}(\omega_{n;1})E^{\alpha_k}(\omega_{n;2})\frac{-\delta}{\delta\gamma_{\boldsymbol{k}a}(\tau)}h^{\alpha_1\alpha_2}_{\boldsymbol{k}aa'}\frac{\delta}{\delta\overline{\alpha}_{\boldsymbol{k}a'}(\tau)}+\cdots\right\}\right]\\
=&\,1-\int_0^{\beta}d\tau\sum_{aa'}\int\frac{d^d\boldsymbol{k}}{(2\pi)^d}i\int d\omega_{n;1}e^{-i\omega_{n;1}\tau}\left(\frac{e}{\omega_{n;1}}\right)E^{\alpha_1}(\omega_{n;1})\frac{-\delta}{\delta\gamma_{\boldsymbol{k}a}(\tau)}h^{\alpha_1}_{\boldsymbol{k}aa'}\frac{\delta}{\delta\overline{\alpha}_{\boldsymbol{k}a'}(\tau)}\\
&\quad-\int_0^{\beta}d\tau\sum_{aa'}\int\frac{d^d\boldsymbol{k}}{(2\pi)^d}\frac{1}{2!}i^2\int d\omega_{n;1}d\omega_{n;2}e^{-i(\omega_{n;1}+\omega_{n;2})\tau}\\
&\qquad\qquad\times\left(\frac{e^2}{\omega_{n;1}\omega_{n;2}}\right)E^{\alpha_1}(\omega_{n;1})E^{\alpha_2}(\omega_{n;2})\frac{-\delta}{\delta\gamma_{\boldsymbol{k}a}(\tau)}h^{\alpha_1\alpha_2}_{\boldsymbol{k}aa'}\frac{\delta}{\delta\overline{\alpha}_{\boldsymbol{k}a'}(\tau)}\\
&\quad+\frac{1}{2!}\int_0^{\beta}d\tau d\tau'\sum_{aa'bb'}\int\frac{d^d\boldsymbol{k}}{(2\pi)^d}\frac{d^d\boldsymbol{k}'}{(2\pi)^d}i^2\int d\omega_{n;1}d\omega_{n;2}e^{-i(\omega_{n;1}\tau+\omega_{n;2}\tau')}\\
&\qquad\qquad\times\left(\frac{e^2}{\omega_{n;1}\omega_{n;2}}\right)E^{\alpha_1}(\omega_{n;1})E^{\alpha_2}(\omega_{n;2})\frac{-\delta}{\delta\gamma_{\boldsymbol{k}a}(\tau)}h^{\alpha_1}_{\boldsymbol{k}aa'}\frac{\delta}{\delta\overline{\alpha}_{\boldsymbol{k}a'}(\tau)}\frac{-\delta}{\delta\gamma_{\boldsymbol{k}'b}(\tau')}h^{\alpha_2}_{\boldsymbol{k}'bb'}\frac{\delta}{\delta\overline{\alpha}_{\boldsymbol{k}'b'}(\tau')}\\
&\quad+\mathcal{O}(E^3).
\end{aligned}
\tag{C36}
$$

As the diagram calculation in quantum field theory, we can express each contribution as diagrams. Here is the summary of representation methods.

- The contraction of $\frac{\delta}{\delta\overline{\alpha}_{\boldsymbol{k}a}(\tau)}$, $\frac{\delta}{\delta\gamma_{\boldsymbol{k}'a'}(\tau')}$ corresponds to the line which is called "propagator".
- Such contraction is replaced by $\frac{\delta}{\delta\overline{\alpha}_{\boldsymbol{k}a}(\tau)}\frac{\delta}{\delta\gamma_{\boldsymbol{k}'a'}(\tau')}\to(2\pi)^d\delta(\boldsymbol{k}-\boldsymbol{k}')\delta_{aa'}G_{\boldsymbol{k}aa}(\tau-\tau')$ [7].
- The coefficient $h^{\alpha_1\cdots\alpha_m}_{\boldsymbol{k}aa'}$ corresponds to the node which is called "vertex".
- Such vertex connects propagators which represents the contraction of its indices.

[7] If $\boldsymbol{k}\neq\boldsymbol{k}'$, then there remains $\overline{\alpha}G$, $G\gamma$ terms which goes to 0 by $\overline{\alpha},\gamma\to0$. The factor $\delta_{aa'}$ comes from (C19). We must exchange the location of functional derivatives (anti-commutation!) and realize the ordering $\delta\overline{\alpha}\,\delta\gamma$ to apply (C28) directly.

- The external field E^{α} and the output current J^{μ} correspond to the line which is called "external line".
- The external line grows from the vertex which has the same vector index.
- The diagram which doesn't contain μ (the vector index of output current J^{μ}) is called "bubble diagram".
- Applying the diagram representation, (C32) becomes,

$$\langle \widehat{J}^{\mu} \rangle(\tau) = \frac{(\text{Bubble diagrams}) \times (\text{Non-bubble diagrams})}{(\text{Bubble diagrams})}. \tag{C37}$$

- Therefore, only we have to do is to calculate the contribution of "non-bubble diagrams".

5. The first order

The corresponding terms in the product of (C35) and (C36) is,

$$\begin{aligned}
&(\mathcal{O}(E)\text{ terms}) \\
&= \left\{ \sum_{aa'} \int \frac{d^d\boldsymbol{k}}{(2\pi)^d} \frac{-\delta}{\delta\gamma_{\boldsymbol{k}a}(\tau)} h^{\mu}_{\boldsymbol{k}aa'} \frac{\delta}{\delta\overline{\alpha}_{\boldsymbol{k}a'}(\tau)} \right\} \\
&\qquad \times \left\{ -\int_0^{\beta} d\tau' \sum_{bb'} \int \frac{d^d\boldsymbol{k'}}{(2\pi)^d} i \int d\omega_{n;1} e^{-i\omega_{n;1}\tau'} \left(\frac{e}{\omega_{n;1}}\right) E^{\alpha_1}(\omega_{n;1}) \frac{-\delta}{\delta\gamma_{\boldsymbol{k'}b}(\tau')} h^{\alpha_1}_{\boldsymbol{k'}bb'} \frac{\delta}{\delta\overline{\alpha}_{\boldsymbol{k'}b'}(\tau')} \right\} \\
&\quad + \left\{ \sum_{aa'} \int \frac{d^d\boldsymbol{k}}{(2\pi)^d} i \int d\omega_{n;1} e^{-i\omega_{n;1}\tau} \left(\frac{e}{\omega_{n;1}}\right) E^{\alpha_1}(\omega_{n;1}) \frac{-\delta}{\delta\gamma_{\boldsymbol{k}a}(\tau)} h^{\mu\alpha_1}_{\boldsymbol{k}aa'} \frac{\delta}{\delta\overline{\alpha}_{\boldsymbol{k}a'}(\tau)} \right\} \times 1 \\
&= \sum_{ab} \int \frac{d^d\boldsymbol{k}}{(2\pi)^d} \int_0^{\beta} d\tau'\, i \int d\omega_{n;1} e^{-i\omega_{n;1}\tau'} \left(\frac{e}{\omega_{n;1}}\right) E^{\alpha_1}(\omega_{n;1}) h^{\mu}_{\boldsymbol{k}ab} G_{\boldsymbol{k}bb}(\tau-\tau') h^{\alpha_1}_{\boldsymbol{k}ba} G_{\boldsymbol{k}aa}(\tau'-\tau) \qquad \text{(C38)} \\
&\quad + \sum_{a} \int \frac{d^d\boldsymbol{k}}{(2\pi)^d} i \int d\omega_{n;1} e^{-i\omega_{n;1}\tau} \left(\frac{e}{\omega_{n;1}}\right) E^{\alpha_1}(\omega_{n;1}) h^{\mu\alpha_1}_{\boldsymbol{k}aa} G_{\boldsymbol{k}aa}(\tau-\tau). \qquad \text{(C39)}
\end{aligned}$$

We perform the inverse Fourier transformation $\langle \widehat{J}^{\mu} \rangle(\omega_n) = \int_0^{\beta} d\tau \langle \widehat{J}^{\mu} \rangle(\tau) e^{i\omega_n\tau}$. Then, the relevant part of τ, τ' integral in (C38) becomes,

$$\int_0^{\beta} d\tau e^{i\omega_n\tau} \int_0^{\beta} d\tau' e^{-i\omega_{n;1}\tau'} G_{\boldsymbol{k}bb}(\tau-\tau') G_{\boldsymbol{k}aa}(\tau'-\tau) = \sum_{n'} \delta_{\omega_n,\omega_{n;1}} \frac{1}{i\omega_{n;1}+i\omega_{n'}-\varepsilon_{\boldsymbol{k}b}} \frac{1}{i\omega_{n'}-\varepsilon_{\boldsymbol{k}a}}. \tag{C40}$$

Similarly, the relevant part of τ, τ' integral in (C39) becomes,

$$\int_0^{\beta} d\tau e^{i\omega_n\tau} e^{-i\omega_{n;1}\tau} G_{\boldsymbol{k}aa}(\tau-\tau) = \sum_{n'} \delta_{\omega_n,\omega_{n;1}} \frac{1}{i\omega_{n'}-\varepsilon_{\boldsymbol{k}a}}. \tag{C41}$$

Therefore, the first order of the output current $\langle \widehat{J}^{\mu} \rangle^{(1)}(\omega_n)$ is,

$$\begin{aligned}
\langle \widehat{J}^{\mu} \rangle^{(1)}(\omega_n) &= e \sum_{ab} \int \frac{d^d\boldsymbol{k}}{(2\pi)^d} i \int d\omega_{n;1} \left(\frac{e}{\omega_{n;1}}\right) E^{\alpha_1}(\omega_{n;1}) \\
&\qquad \times \sum_{n'} \delta_{\omega_n,\omega_{n;1}} \left[h^{\mu}_{\boldsymbol{k}ab} h^{\alpha_1}_{\boldsymbol{k}ba} \frac{1}{i\omega_{n;1}+i\omega_{n'}-\varepsilon_{\boldsymbol{k}b}} \frac{1}{i\omega_{n'}-\varepsilon_{\boldsymbol{k}a}} + h^{\mu\alpha_1}_{\boldsymbol{k}aa} \frac{1}{i\omega_{n'}-\varepsilon_{\boldsymbol{k}a}} \right].
\end{aligned} \tag{C42}$$

6. The second order

The corresponding terms in the product of (C35) and (C36) is,

$$
\begin{aligned}
&(\mathcal{O}(E^2)\text{ terms})\\
=&\sum_{aa'}\int\frac{d^d\boldsymbol{k}}{(2\pi)^d}\left\{\frac{-\delta}{\delta\gamma_{\boldsymbol{k}a}(\tau)}h^{\mu}_{\boldsymbol{k}aa'}\frac{\delta}{\delta\overline{\alpha}_{\boldsymbol{k}a'}(\tau)}\right\}\\
&\times\left\{\frac{1}{2!}\int_0^\beta d\tau' d\tau''\sum_{bb'cc'}\int\frac{d^d\boldsymbol{k'}}{(2\pi)^d}\frac{d^d\boldsymbol{k''}}{(2\pi)^d}i^2\int d\omega_{n;1}d\omega_{n;2}e^{-i(\omega_{n;1}\tau'+\omega_{n;2}\tau'')}\right.\\
&\left.\times\left(\frac{e^2}{\omega_{n;1}\omega_{n;2}}\right)E^{\alpha_1}(\omega_{n;1})E^{\alpha_2}(\omega_{n;2})\frac{-\delta}{\delta\gamma_{\boldsymbol{k'}b}(\tau')}h^{\alpha_1}_{\boldsymbol{k'}bb'}\frac{\delta}{\delta\overline{\alpha}_{\boldsymbol{k'}b'}(\tau')}\frac{-\delta}{\delta\gamma_{\boldsymbol{k''}c}(\tau'')}h^{\alpha_2}_{\boldsymbol{k''}cc'}\frac{\delta}{\delta\overline{\alpha}_{\boldsymbol{k''}c'}(\tau'')}\right\}\\
&-\sum_{aa'}\int\frac{d^d\boldsymbol{k}}{(2\pi)^d}\left\{\frac{-\delta}{\delta\gamma_{\boldsymbol{k}a}(\tau)}h^{\mu}_{\boldsymbol{k}aa'}\frac{\delta}{\delta\overline{\alpha}_{\boldsymbol{k}a'}(\tau)}\right\}\\
&\times\left\{\int_0^\beta d\tau'\sum_{bb'}\int\frac{d^d\boldsymbol{k'}}{(2\pi)^d}\frac{1}{2!}i^2\int d\omega_{n;1}d\omega_{n;2}e^{-i(\omega_{n;1}+\omega_{n;2})\tau'}\right.\\
&\left.\times\left(\frac{e^2}{\omega_{n;1}\omega_{n;2}}\right)E^{\alpha_1}(\omega_{n;1})E^{\alpha_2}(\omega_{n;2})\frac{-\delta}{\delta\gamma_{\boldsymbol{k'}b}(\tau')}h^{\alpha_1\alpha_2}_{\boldsymbol{k'}bb'}\frac{\delta}{\delta\overline{\alpha}_{\boldsymbol{k'}b'}(\tau')}\right\}\\
&-\sum_{aa'}\int\frac{d^d\boldsymbol{k}}{(2\pi)^d}\left\{i\int d\omega_{n;1}e^{-i\omega_{n;1}\tau}\left(\frac{e}{\omega_{n;1}}\right)E^{\alpha_1}(\omega_{n;1})\frac{-\delta}{\delta\gamma_{\boldsymbol{k}a}(\tau)}h^{\mu\alpha_1}_{\boldsymbol{k}aa'}\frac{\delta}{\delta\overline{\alpha}_{\boldsymbol{k}a'}(\tau)}\right\}\\
&\times\left\{\int_0^\beta d\tau'\sum_{bb'}\int\frac{d^d\boldsymbol{k'}}{(2\pi)^d}i\int d\omega_{n;2}e^{-i\omega_{n;2}\tau'}\left(\frac{e}{\omega_{n;2}}\right)E^{\alpha_2}(\omega_{n;2})\frac{-\delta}{\delta\gamma_{\boldsymbol{k'}b'}(\tau')}h^{\alpha_2}_{\boldsymbol{k'}bb'}\frac{\delta}{\delta\overline{\alpha}_{\boldsymbol{k'}b}(\tau')}\right\}\\
&+\sum_{aa'}\int\frac{d^d\boldsymbol{k}}{(2\pi)^d}\left\{\frac{1}{2!}i^2\int d\omega_{n;1}d\omega_{n;2}e^{-i(\omega_{n;1}+\omega_{n;2})\tau}\right.\\
&\left.\times\left(\frac{e^2}{\omega_{n;1}\omega_{n;2}}\right)E^{\alpha_1}(\omega_{n;1})E^{\alpha_2}(\omega_{n;2})\frac{-\delta}{\delta\gamma_{\boldsymbol{k}a'}(\tau)}h^{\mu\alpha_1\alpha_2}_{\boldsymbol{k}aa'}\frac{\delta}{\delta\overline{\alpha}_{\boldsymbol{k}a}(\tau)}\right\}\times 1\\
=&\frac{1}{2!}\sum_{abc}\int\frac{d^d\boldsymbol{k}}{(2\pi)^d}\int_0^\beta d\tau' d\tau''\,i^2\int d\omega_{n;1}d\omega_{n;2}e^{-i(\omega_{n;1}\tau'+\omega_{n;2}\tau'')}\\
&\times\left(\frac{e^2}{\omega_{n;1}\omega_{n;2}}\right)E^{\alpha_1}(\omega_{n;1})E^{\alpha_2}(\omega_{n;2})h^{\mu}_{\boldsymbol{k}ab}G_{\boldsymbol{k}bb}(\tau-\tau')h^{\alpha_1}_{\boldsymbol{k}bc}G_{\boldsymbol{k}cc}(\tau'-\tau'')h^{\alpha_2}_{\boldsymbol{k}ca}G_{\boldsymbol{k}aa}(\tau''-\tau) &&\text{(C43)}\\
&+[(\omega_{n;1},\alpha_1)\longleftrightarrow(\omega_{n;2},\alpha_2)]\\
&+\frac{1}{2!}\sum_{ab}\int\frac{d^d\boldsymbol{k}}{(2\pi)^d}\int_0^\beta d\tau'\,i^2\int d\omega_{n;1}d\omega_{n;2}e^{-i(\omega_{n;1}+\omega_{n;2})\tau'}\\
&\times\left(\frac{e^2}{\omega_{n;1}\omega_{n;2}}\right)E^{\alpha_1}(\omega_{n;1})E^{\alpha_2}(\omega_{n;2})h^{\mu}_{\boldsymbol{k}ab}G_{\boldsymbol{k}bb}(\tau-\tau')h^{\alpha_1\alpha_2}_{\boldsymbol{k}ba}G_{\boldsymbol{k}aa}(\tau'-\tau) &&\text{(C44)}\\
&+\sum_{ab}\int\frac{d^d\boldsymbol{k}}{(2\pi)^d}\int_0^\beta d\tau'\,i^2\int d\omega_{n;1}d\omega_{n;2}e^{-i(\omega_{n;1}\tau+\omega_{n;2}\tau')}\\
&\times\left(\frac{e^2}{\omega_{n;1}\omega_{n;2}}\right)E^{\alpha_1}(\omega_{n;1})E^{\alpha_2}(\omega_{n;2})h^{\mu\alpha_1}_{\boldsymbol{k}ab}G_{\boldsymbol{k}bb}(\tau-\tau')h^{\alpha_2}_{\boldsymbol{k}ba}G_{\boldsymbol{k}aa}(\tau'-\tau) &&\text{(C45)}\\
&+\frac{1}{2!}\sum_{a}\int\frac{d^d\boldsymbol{k}}{(2\pi)^d}i^2\int d\omega_{n;1}d\omega_{n;2}e^{-i(\omega_{n;1}+\omega_{n;2})\tau}\\
&\times\left(\frac{e^2}{\omega_{n;1}\omega_{n;2}}\right)E^{\alpha_1}(\omega_{n;1})E^{\alpha_2}(\omega_{n;2})h^{\mu\alpha_1\alpha_2}_{\boldsymbol{k}aa}G_{\boldsymbol{k}aa}(\tau-\tau). &&\text{(C46)}
\end{aligned}
$$

Performing the inverse Fourier transformation $\langle \widehat{J}^\mu\rangle(\omega_n) = \int_0^\beta d\tau \langle \widehat{J}^\mu\rangle(\tau) e^{i\omega_n\tau}$, the relevant part of τ, τ' integral in (C43) becomes,

$$\begin{aligned}
&\int_0^\beta d\tau e^{i\omega_n\tau}\int_0^\beta d\tau' d\tau''\, e^{-i(\omega_{n;1}\tau'+\omega_{n;2}\tau'')} G_{\boldsymbol{k}bb}(\tau-\tau')G_{\boldsymbol{k}cc}(\tau'-\tau'')G_{\boldsymbol{k}aa}(\tau''-\tau)\\
&=\sum_{n'}\delta_{\omega_n,\omega_{n;2}+\omega_{n;1}}\frac{1}{i(\omega_{n;1}+\omega_{n;2}+\omega_{n'})-\varepsilon_{\boldsymbol{k}b}}\frac{1}{i(\omega_{n;2}+\omega_{n'})-\varepsilon_{\boldsymbol{k}c}}\frac{1}{i\omega_{n'}-\varepsilon_{\boldsymbol{k}a}}.
\end{aligned}\tag{C47}$$

Similarly, for (C44),

$$\begin{aligned}
&\int_0^\beta d\tau e^{i\omega_n\tau}\int_0^\beta d\tau'\, e^{-i(\omega_{n;1}+\omega_{n;2})\tau'} G_{\boldsymbol{k}bb}(\tau-\tau')G_{\boldsymbol{k}aa}(\tau'-\tau)\\
&=\sum_{n'}\delta_{\omega_n,\omega_{n;1}+\omega_{n;2}}\frac{1}{i(\omega_{n;1}+\omega_{n;2}+\omega_{n'})-\varepsilon_{\boldsymbol{k}b}}\frac{1}{i\omega_{n'}-\varepsilon_{\boldsymbol{k}a}}.
\end{aligned}\tag{C48}$$

For (C45),

$$\begin{aligned}
&\int_0^\beta d\tau e^{i\omega_n\tau}\int_0^\beta d\tau'\, e^{-i(\omega_{n;1}\tau+\omega_{n;2}\tau')} G_{\boldsymbol{k}bb}(\tau-\tau')G_{\boldsymbol{k}aa}(\tau'-\tau)\\
&=\sum_{n'}\delta_{\omega_n,\omega_{n;1}+\omega_{n;2}}\frac{1}{i(\omega_{n;2}+\omega_{n'})-\varepsilon_{\boldsymbol{k}b}}\frac{1}{i\omega_{n'}-\varepsilon_{\boldsymbol{k}a}}.
\end{aligned}\tag{C49}$$

For (C46),

$$\int_0^\beta d\tau e^{i\omega_n\tau} e^{-i(\omega_{n;1}+\omega_{n;2})\tau} G_{\boldsymbol{k}aa}(\tau-\tau) = \sum_{n'}\delta_{\omega_n,\omega_{n;1}+\omega_{n;2}}\frac{1}{i\omega_{n'}-\varepsilon_{\boldsymbol{k}a}}.\tag{C50}$$

Therefore, the second order of the output current $\langle \widehat{J}^\mu\rangle^{(2)}(\omega_n)$ is,

$$\begin{aligned}
\langle \widehat{J}^\mu\rangle^{(2)}(\omega_n) = {}& e\frac{1}{2!}\sum_{abc}\int\frac{d^d\boldsymbol{k}}{(2\pi)^d} i^2\int d\omega_{n;1}d\omega_{n;2}\left(\frac{e^2}{\omega_{n;1}\omega_{n;2}}\right)E^{\alpha_1}(\omega_{n;1})E^{\alpha_2}(\omega_{n;2})\sum_{n'}\delta_{\omega_n,\omega_{n;1}+\omega_{n;2}}\\
&\times h^\mu_{\boldsymbol{k}ab}h^{\alpha_1}_{\boldsymbol{k}bc}h^{\alpha_2}_{\boldsymbol{k}ca}\frac{1}{i(\omega_{n;1}+\omega_{n;2}+\omega_{n'})-\varepsilon_{\boldsymbol{k}b}}\frac{1}{i(\omega_{n;2}+\omega_{n'})-\varepsilon_{\boldsymbol{k}c}}\frac{1}{i\omega_{n'}-\varepsilon_{\boldsymbol{k}a}}\\
&+[(\omega_{n;1},\alpha_1)\longleftrightarrow(\omega_{n;2},\alpha_2)]\\
&+e\frac{1}{2!}\sum_{ab}\int\frac{d^d\boldsymbol{k}}{(2\pi)^d} i^2\int d\omega_{n;1}d\omega_{n;2}\left(\frac{e^2}{\omega_{n;1}\omega_{n;2}}\right)\sum_{n'}\delta_{\omega_n,\omega_{n;1}+\omega_{n;2}}E^{\alpha_1}(\omega_{n;1})E^{\alpha_2}(\omega_{n;2})\\
&\times h^\mu_{\boldsymbol{k}ab}h^{\alpha_1\alpha_2}_{\boldsymbol{k}ba}\frac{1}{i(\omega_{n;1}+\omega_{n;2}+\omega_{n'})-\varepsilon_{\boldsymbol{k}b}}\frac{1}{i\omega_{n'}-\varepsilon_{\boldsymbol{k}a}}\\
&+e\sum_{ab}\int\frac{d^d\boldsymbol{k}}{(2\pi)^d} i^2\int d\omega_{n;1}d\omega_{n;2}\left(\frac{e^2}{\omega_{n;1}\omega_{n;2}}\right)E^{\alpha_1}(\omega_{n;1})E^{\alpha_2}(\omega_{n;2})\sum_{n'}\delta_{\omega_n,\omega_{n;1}+\omega_{n;2}}\\
&\times h^{\mu\alpha_1}_{\boldsymbol{k}ab}h^{\alpha_2}_{\boldsymbol{k}ba}\frac{1}{i(\omega_{n;2}+\omega_{n'})-\varepsilon_{\boldsymbol{k}b}}\frac{1}{i\omega_{n'}-\varepsilon_{\boldsymbol{k}a}}\\
&+e\frac{1}{2!}\sum_{a}\int\frac{d^d\boldsymbol{k}}{(2\pi)^d} i^2\int d\omega_{n;1}d\omega_{n;2}\left(\frac{e^2}{\omega_{n;1}\omega_{n;2}}\right)E^{\alpha_1}(\omega_{n;1})E^{\alpha_2}(\omega_{n;2})\sum_{n'}\delta_{\omega_n,\omega_{n;1}+\omega_{n;2}}\\
&\times h^{\mu\alpha_1\alpha_2}_{\boldsymbol{k}aa}\frac{1}{i\omega_{n'}-\varepsilon_{\boldsymbol{k}a}}.
\end{aligned}\tag{C51}$$

Finally, we go back to the $\{t,\omega\}$ representation,

$$
\begin{aligned}
\langle\widehat{J}^{\mu}\rangle^{(2)}(\omega)=e\frac{1}{2!}\sum_{abc}\int\frac{d^d\boldsymbol{k}}{(2\pi)^d}\int d\omega_1 d\omega_2\left(\frac{i^2e^2}{\omega_1\omega_2}\right)E^{\alpha_1}(\omega_1)E^{\alpha_2}(\omega_2)\int d\omega'\delta(\omega-\omega_1-\omega_2)\\
\times h^{\mu}_{\boldsymbol{k}ab}h^{\alpha_1}_{\boldsymbol{k}bc}h^{\alpha_2}_{\boldsymbol{k}ca}\frac{1}{(\omega_1+\omega_2+\omega')-\varepsilon_{\boldsymbol{k}b}}\frac{1}{(\omega_2+\omega')-\varepsilon_{\boldsymbol{k}c}}\frac{1}{\omega'-\varepsilon_{\boldsymbol{k}a}}\\
+e\frac{1}{2}\frac{1}{2!}\sum_{ab}\int\frac{d^d\boldsymbol{k}}{(2\pi)^d}\int d\omega_1 d\omega_2\left(\frac{i^2e^2}{\omega_1\omega_2}\right)\int d\omega'\delta(\omega-\omega_1-\omega_2)E^{\alpha_1}(\omega_1)E^{\alpha_2}(\omega_2)\\
\times h^{\mu}_{\boldsymbol{k}ab}h^{\alpha_1\alpha_2}_{\boldsymbol{k}ba}\frac{1}{(\omega_1+\omega_2+\omega')-\varepsilon_{\boldsymbol{k}b}}\frac{1}{\omega'-\varepsilon_{\boldsymbol{k}a}}\\
+e\frac{1}{2}\sum_{ab}\int\frac{d^d\boldsymbol{k}}{(2\pi)^d}\int d\omega_1 d\omega_2\left(\frac{i^2e^2}{\omega_1\omega_2}\right)E^{\alpha_1}(\omega_1)E^{\alpha_2}(\omega_2)\int d\omega'\delta(\omega-\omega_1-\omega_2)\\
\times h^{\mu\alpha_1}_{\boldsymbol{k}ab}h^{\alpha_2}_{\boldsymbol{k}ba}\frac{1}{(\omega_2+\omega')-\varepsilon_{\boldsymbol{k}b}}\frac{1}{\omega'-\varepsilon_{\boldsymbol{k}a}}\\
+e\frac{1}{2}\frac{1}{2!}\sum_{a}\int\frac{d^d\boldsymbol{k}}{(2\pi)^d}\int d\omega_1 d\omega_2\left(\frac{i^2e^2}{\omega_1\omega_2}\right)E^{\alpha_1}(\omega_1)E^{\alpha_2}(\omega_2)\int d\omega'\delta(\omega-\omega_1-\omega_2)\\
\times h^{\mu\alpha_1\alpha_2}_{\boldsymbol{k}aa}\frac{1}{\omega'-\varepsilon_{\boldsymbol{k}a}}\\
+[(\omega_1,\alpha_1)\longleftrightarrow(\omega_2,\alpha_2)],
\end{aligned}
\tag{C52}
$$

where we symmetrized all of the terms. That is the reason that the factor "1/2" is added on the latter three terms and the position of "$[(\omega_1,\alpha_1)\longleftrightarrow(\omega_2,\alpha_2)]$" is changed to the bottom. Here's the integration formula:

$$I_1=\int d\omega'\frac{1}{\omega'-\varepsilon_{\boldsymbol{k}a}}=f_a \tag{C53}$$

$$I_2(\omega_1)=\int d\omega'\frac{1}{\omega'-\varepsilon_{\boldsymbol{k}a}}\frac{1}{\omega'+\omega_1-\varepsilon_{\boldsymbol{k}b}}=\frac{f_{ab}}{\omega_1-\varepsilon_{\boldsymbol{k}ba}} \tag{C54}$$

$$I_3(\omega_1,\omega_2)=\int d\omega'\frac{1}{\omega'-\varepsilon_{\boldsymbol{k}a}}\frac{1}{\omega'+\omega_1-\varepsilon_{\boldsymbol{k}b}}\frac{1}{\omega'+\omega_1+\omega_2-\varepsilon_{\boldsymbol{k}c}}=\frac{(\omega_2-\varepsilon_{\boldsymbol{k}cb})f_{ab}+(\omega_1-\varepsilon_{\boldsymbol{k}ba})f_{cb}}{(\omega_1-\varepsilon_{\boldsymbol{k}ba})(\omega_2-\varepsilon_{\boldsymbol{k}cb})(\omega-\varepsilon_{\boldsymbol{k}ca})}, \tag{C55}$$

where $f_a=f(\varepsilon_{\boldsymbol{k}a})=\frac{1}{\exp(\beta\varepsilon_{\boldsymbol{k}a})+1}$ is the Fermi factor in the finite inverse temperature β and $f_{ab}=f_a-f_b$, $\varepsilon_{\boldsymbol{k}ab}=\varepsilon_{\boldsymbol{k}a}-\varepsilon_{\boldsymbol{k}b}$ are differences of Fermi factors and energies, and $\omega=\omega_1+\omega_2$. Using them, the current becomes,

$$
\begin{aligned}
\langle\widehat{J}^{\mu}\rangle^{(2)}(\omega)=\ &\frac{1}{2}\sum_{abc}\int\frac{d^d\boldsymbol{k}}{(2\pi)^d}\int d\omega_1 d\omega_2\left(\frac{-e^3}{\omega_1\omega_2}\right)E^{\alpha_1}(\omega_1)E^{\alpha_2}(\omega_2)\delta(\omega-\omega_1-\omega_2)\\
\times&\left[h^{\mu}_{\boldsymbol{k}ac}h^{\alpha_1}_{\boldsymbol{k}cb}h^{\alpha_2}_{\boldsymbol{k}ba}\frac{(\omega_1-\varepsilon_{\boldsymbol{k}cb})f_{ab}+(\omega_2-\varepsilon_{\boldsymbol{k}ba})f_{cb}}{(\omega_2-\varepsilon_{\boldsymbol{k}ba})(\omega_1-\varepsilon_{\boldsymbol{k}cb})(\omega-\varepsilon_{\boldsymbol{k}ca})}+\frac{1}{2}h^{\mu}_{\boldsymbol{k}ab}h^{\alpha_1\alpha_2}_{\boldsymbol{k}ba}\frac{f_{ab}}{\omega_1+\omega_2-\varepsilon_{\boldsymbol{k}ba}}\right.\\
&\left.+h^{\mu\alpha_1}_{\boldsymbol{k}ab}h^{\alpha_2}_{\boldsymbol{k}ba}\frac{f_{ab}}{\omega_2-\varepsilon_{\boldsymbol{k}ba}}+\frac{1}{2}h^{\mu\alpha_1\alpha_2}_{\boldsymbol{k}aa}f_a+[(\omega_1,\alpha_1)\longleftrightarrow(\omega_2,\alpha_2)]\right],
\end{aligned}
\tag{C56}
$$

To get $h^{\alpha_1\cdots\alpha_n}_{\boldsymbol{k}aa'}$, we need to calculate the k-dependent form of covariant derivative $\widehat{h}^{\alpha_1\cdots\alpha_n}(\boldsymbol{k})=\widehat{\mathcal{D}}^{\alpha_1}\cdots\widehat{\mathcal{D}}^{\alpha_n}[\widehat{H}_0](\boldsymbol{k})$. Operating $\widehat{\boldsymbol{\mathcal{D}}}$ to $\widehat{\mathcal{O}}$ once,

$$
\begin{aligned}
\widehat{\boldsymbol{\mathcal{D}}}[\widehat{\mathcal{O}}](\boldsymbol{k})=&e^{-i\boldsymbol{k}\cdot\boldsymbol{r}}[-i\,\widehat{\boldsymbol{r}},\ \widehat{\mathcal{O}}]e^{i\boldsymbol{k}\cdot\boldsymbol{r}}\\
=&e^{-i\boldsymbol{k}\cdot\boldsymbol{r}}\widehat{\mathcal{O}}\,i\,\widehat{\boldsymbol{r}}e^{i\boldsymbol{k}\cdot\boldsymbol{r}}-e^{-i\boldsymbol{k}\cdot\boldsymbol{r}}i\,\widehat{\boldsymbol{r}}\widehat{\mathcal{O}}e^{i\boldsymbol{k}\cdot\boldsymbol{r}}\\
=&e^{-i\boldsymbol{k}\cdot\boldsymbol{r}}\widehat{\mathcal{O}}\left(\frac{\partial}{\partial\boldsymbol{k}}e^{i\boldsymbol{k}\cdot\boldsymbol{r}}\right)+\left(\frac{\partial}{\partial\boldsymbol{k}}e^{-i\boldsymbol{k}\cdot\boldsymbol{r}}\right)\widehat{\mathcal{O}}e^{i\boldsymbol{k}\cdot\boldsymbol{r}}\\
=&\frac{\partial}{\partial\boldsymbol{k}}\widehat{\mathcal{O}}(\boldsymbol{k}).
\end{aligned}
\tag{C57}
$$

Operating $\widehat{\boldsymbol{\mathcal{D}}}$ to $\widehat{\mathcal{O}}$ twice,

$$\widehat{\boldsymbol{\mathcal{D}}}[\widehat{\boldsymbol{\mathcal{D}}}[\widehat{\mathcal{O}}]](\boldsymbol{k})=\frac{\partial}{\partial\boldsymbol{k}}\left(\widehat{\boldsymbol{\mathcal{D}}}[\widehat{\mathcal{O}}](\boldsymbol{k})\right)=\frac{\partial}{\partial\boldsymbol{k}}\frac{\partial}{\partial\boldsymbol{k}}\widehat{\mathcal{O}}(\boldsymbol{k}). \tag{C58}$$

Therefore, in k-dependent form, we can treat $\widehat{\boldsymbol{\mathcal{D}}}$ as k-derivative.

$$\widehat{h}^{\alpha_1 \dots \alpha_n}(\boldsymbol{k}) = \partial_{k^{\alpha_1}} \cdots \partial_{k^{\alpha_n}} \widehat{H}_0(\boldsymbol{k}). \tag{C59}$$

Its matrix element is,

$$h^{\alpha_1 \dots \alpha_n}_{\boldsymbol{k}aa'} = \langle u_{\boldsymbol{k}a'} | \partial_{k^{\alpha_1}} \cdots \partial_{k^{\alpha_n}} \widehat{H}_0(\boldsymbol{k}) | u_{\boldsymbol{k}a} \rangle_V. \tag{C60}$$

To describe it in terms of Berry connection $\mathcal{A}^{\mu}_{ab}(\boldsymbol{k})$, we use the following relation:

$$\langle \psi_{\boldsymbol{k}a} | \mathcal{D}^{\mu}(\boldsymbol{k}) | \psi_{\boldsymbol{k}b} \rangle = \langle \psi_{\boldsymbol{k}a} | \left(\delta_{ab} \partial_{k^{\mu}} - i \mathcal{A}^{\mu}(\boldsymbol{k}) \right) | \psi_{\boldsymbol{k}b} \rangle. \tag{C61}$$

Then, for $h^{\mu}_{\boldsymbol{k}ab}$,

$$\begin{aligned} h^{\mu}_{\boldsymbol{k}ab} =& \langle \psi_{\boldsymbol{k}a} | \left[\mathcal{D}^{\mu}(\boldsymbol{k}),\, \widehat{H}_0 \right] | \psi_{\boldsymbol{k}b} \rangle \\ =& \langle \psi_{\boldsymbol{k}a} | \left(\delta_{ab} \partial_{k^{\mu}} - i \mathcal{A}^{\mu}(\boldsymbol{k}) \right) | \psi_{\boldsymbol{k}b} \rangle \varepsilon_{\boldsymbol{k}b} - \varepsilon_{\boldsymbol{k}a} \langle \psi_{\boldsymbol{k}a} | \left(\delta_{ab} \partial_{k^{\mu}} - i \mathcal{A}^{\mu}(\boldsymbol{k}) \right) | \psi_{\boldsymbol{k}b} \rangle \\ =& \delta_{ab} \partial_{k^{\mu}} \varepsilon_{\boldsymbol{k}a} + i \varepsilon_{\boldsymbol{k}ab} \mathcal{A}^{\mu}_{ab}(\boldsymbol{k}). \end{aligned} \tag{C62}$$

For $h^{\mu\alpha}_{\boldsymbol{k}ab}$,

$$\begin{aligned} h^{\mu\alpha}_{\boldsymbol{k}ab} =& \langle \psi_{\boldsymbol{k}a} | \left[\mathcal{D}^{\mu}(\boldsymbol{k}),\, \widehat{h}^{\alpha} \right] | \psi_{\boldsymbol{k}b} \rangle \\ =& \langle \psi_{\boldsymbol{k}a} | \mathcal{D}^{\mu}(\boldsymbol{k}) | \psi_{\boldsymbol{k}c} \rangle \langle \psi_{\boldsymbol{k}c} | \widehat{h}^{\alpha} | \psi_{\boldsymbol{k}b} \rangle - \langle \psi_{\boldsymbol{k}a} | \widehat{h}^{\alpha} | \psi_{\boldsymbol{k}c} \rangle \langle \psi_{\boldsymbol{k}c} | \mathcal{D}^{\mu}(\boldsymbol{k}) | \psi_{\boldsymbol{k}b} \rangle \\ =& \langle \psi_{\boldsymbol{k}a} | \left(\delta_{ac} \partial_{k^{\mu}} - i \mathcal{A}^{\mu}(\boldsymbol{k}) \right) | \psi_{\boldsymbol{k}c} \rangle h^{\alpha}_{\boldsymbol{k}cb} - h^{\alpha}_{\boldsymbol{k}ac} \langle \psi_{\boldsymbol{k}c} | \left(\delta_{cb} \partial_{k^{\mu}} - i \mathcal{A}^{\mu}(\boldsymbol{k}) \right) | \psi_{\boldsymbol{k}b} \rangle \\ =& \partial_{k^{\mu}} h^{\alpha}_{\boldsymbol{k}ab} - i \mathcal{A}^{\mu}_{ac}(\boldsymbol{k}) h^{\alpha}_{\boldsymbol{k}cb} + i h^{\alpha}_{\boldsymbol{k}ac} \mathcal{A}^{\mu}_{cb}(\boldsymbol{k}). \end{aligned} \tag{C63}$$

7. Shift current

Shift current is the γ independent part of the second order response. It is obtained from the contribution satisfying $a \neq c$. We assume that γ, ω is sufficiently small compared to the energy scale of the system. Then the resonant contribution (ω_1, $\omega_2 \sim \varepsilon_{\boldsymbol{k}ab}$) is,

$$\begin{aligned} &\langle \widehat{J}^{\mu}_{\text{shift}} \rangle^{(2)}(\omega) \\ &= \frac{1}{2} \sum_{abcd(a\neq c)} \int \frac{d^d\boldsymbol{k}}{(2\pi)^d} \int d\omega_1 d\omega_2 \left(\frac{-e^3}{\omega_1 \omega_2} \right) E^{\alpha_1}(\omega_1) E^{\alpha_2}(\omega_2) \delta(\omega - \omega_1 - \omega_2) \\ &\quad \times \Bigg[h^{\mu}_{\boldsymbol{k}ac} h^{\alpha_1}_{\boldsymbol{k}cb} h^{\alpha_2}_{\boldsymbol{k}ba} \frac{f_{ab}}{(\omega_2 - \varepsilon_{\boldsymbol{k}ba} + i\gamma)(-\varepsilon_{\boldsymbol{k}ca})} + h^{\mu}_{\boldsymbol{k}ac} h^{\alpha_1}_{\boldsymbol{k}cb} h^{\alpha_2}_{\boldsymbol{k}ba} \frac{f_{cb}}{(\omega_1 - \varepsilon_{\boldsymbol{k}cb} + i\gamma)(-\varepsilon_{\boldsymbol{k}ca})} \\ &\qquad + h^{\mu\alpha_1}_{\boldsymbol{k}ab} h^{\alpha_2}_{\boldsymbol{k}ba} \frac{f_{ab}}{\omega_2 - \varepsilon_{\boldsymbol{k}ba} + i\gamma} + [(\omega_1, \alpha_1) \longleftrightarrow (\omega_2, \alpha_2)] \Bigg] \\ &= \frac{1}{2} \sum_{abcd(a\neq c)} \int \frac{d^d\boldsymbol{k}}{(2\pi)^d} \int d\omega_1 d\omega_2 \left(\frac{-e^3}{\omega_1 \omega_2} \right) E^{\alpha_1}(\omega_1) E^{\alpha_2}(\omega_2) \delta(\omega - \omega_1 - \omega_2) \\ &\quad \times \Bigg[i \mathcal{A}^{\mu}_{ac}(\boldsymbol{k}) h^{\alpha_1}_{\boldsymbol{k}cb} h^{\alpha_2}_{\boldsymbol{k}ba} \frac{f_{ab}}{\omega_2 - \varepsilon_{\boldsymbol{k}ba} + i\gamma} + i \mathcal{A}^{\mu}_{ac}(\boldsymbol{k}) h^{\alpha_1}_{\boldsymbol{k}cb} h^{\alpha_2}_{\boldsymbol{k}ba} \frac{f_{cb}}{\omega_1 - \varepsilon_{\boldsymbol{k}cb} + i\gamma} + \partial_{k^{\mu}} h^{\alpha_1}_{\boldsymbol{k}ab} h^{\alpha_2}_{\boldsymbol{k}ba} \frac{f_{ab}}{\omega_2 - \varepsilon_{\boldsymbol{k}ba} + i\gamma} \\ &\qquad - i \mathcal{A}^{\mu}_{ad}(\boldsymbol{k}) h^{\alpha_1}_{\boldsymbol{k}db} h^{\alpha_2}_{\boldsymbol{k}ba} \frac{f_{ab}}{\omega_2 - \varepsilon_{\boldsymbol{k}ba} + i\gamma} + i h^{\alpha_1}_{\boldsymbol{k}ad} \mathcal{A}^{\mu}_{db}(\boldsymbol{k}) h^{\alpha_2}_{\boldsymbol{k}ba} \frac{f_{ab}}{\omega_2 - \varepsilon_{\boldsymbol{k}ba} + i\gamma} + [(\omega_1, \alpha_1) \longleftrightarrow (\omega_2, \alpha_2)] \Bigg], \end{aligned} \tag{C64}$$

where we have used (C62), (C63). The summation over d is decomposed into $d = a$ part and $d \neq a$ part. Then, for $d \neq a$ part, dummy variables d and c play the same role in the expression. Therefore they are merged into a single variable c to continue the calculation:

$$
\begin{aligned}
&\langle \widehat{J}^{\mu}_{\rm shift}\rangle^{(2)}(\omega)\\
&=\frac{1}{2}\sum_{abc(a\neq c)}\int\frac{d^d\boldsymbol{k}}{(2\pi)^d}\int d\omega_1 d\omega_2\left(\frac{-e^3}{\omega_1\omega_2}\right)E^{\alpha_1}(\omega_1)E^{\alpha_2}(\omega_2)\delta(\omega-\omega_1-\omega_2)\\
&\quad\times\Bigg[i\mathcal{A}^{\mu}_{ac}(\boldsymbol{k})h^{\alpha_1}_{\boldsymbol{k}cb}h^{\alpha_2}_{\boldsymbol{k}ba}\frac{f_{ab}}{\omega_2-\varepsilon_{\boldsymbol{k}ba}+i\gamma}+i\mathcal{A}^{\mu}_{ac}(\boldsymbol{k})h^{\alpha_1}_{\boldsymbol{k}cb}h^{\alpha_2}_{\boldsymbol{k}ba}\frac{f_{cb}}{\omega_1-\varepsilon_{\boldsymbol{k}cb}+i\gamma}\\
&\qquad+\partial_{k^\mu}h^{\alpha_1}_{\boldsymbol{k}ab}h^{\alpha_2}_{\boldsymbol{k}ba}\frac{f_{ab}}{\omega_2-\varepsilon_{\boldsymbol{k}ba}+i\gamma}-i\mathcal{A}^{\mu}_{aa}(\boldsymbol{k})h^{\alpha_1}_{\boldsymbol{k}ab}h^{\alpha_2}_{\boldsymbol{k}ba}\frac{f_{ab}}{\omega_2-\varepsilon_{\boldsymbol{k}ba}+i\gamma}+ih^{\alpha_1}_{\boldsymbol{k}aa}\mathcal{A}^{\mu}_{ab}(\boldsymbol{k})h^{\alpha_2}_{\boldsymbol{k}ba}\frac{f_{ab}}{\omega_2-\varepsilon_{\boldsymbol{k}ba}+i\gamma}\\
&\qquad-i\mathcal{A}^{\mu}_{ac}(\boldsymbol{k})h^{\alpha_1}_{\boldsymbol{k}cb}h^{\alpha_2}_{\boldsymbol{k}ba}\frac{f_{ab}}{\omega_2-\varepsilon_{\boldsymbol{k}ba}+i\gamma}+ih^{\alpha_1}_{\boldsymbol{k}ac}\mathcal{A}^{\mu}_{cb}(\boldsymbol{k})h^{\alpha_2}_{\boldsymbol{k}ba}\frac{f_{ab}}{\omega_2-\varepsilon_{\boldsymbol{k}ba}+i\gamma}+[(\omega_1,\alpha_1)\longleftrightarrow(\omega_2,\alpha_2)]\Bigg]\\
&=\frac{1}{2}\sum_{abc(a\neq c)}\int\frac{d^d\boldsymbol{k}}{(2\pi)^d}\int d\omega_1 d\omega_2\left(\frac{-e^3}{\omega_1\omega_2}\right)E^{\alpha_1}(\omega_1)E^{\alpha_2}(\omega_2)\delta(\omega-\omega_1-\omega_2)\\
&\quad\times\Bigg[i\mathcal{A}^{\mu}_{ca}(\boldsymbol{k})h^{\alpha_1}_{\boldsymbol{k}ab}h^{\alpha_2}_{\boldsymbol{k}bc}\frac{f_{ab}}{\omega_1-\varepsilon_{\boldsymbol{k}ab}+i\gamma}+\partial_{k^\mu}h^{\alpha_1}_{\boldsymbol{k}ab}h^{\alpha_2}_{\boldsymbol{k}ba}\frac{f_{ab}}{\omega_2-\varepsilon_{\boldsymbol{k}ba}+i\gamma}-i\mathcal{A}^{\mu}_{aa}(\boldsymbol{k})h^{\alpha_1}_{\boldsymbol{k}ab}h^{\alpha_2}_{\boldsymbol{k}ba}\frac{f_{ab}}{\omega_2-\varepsilon_{\boldsymbol{k}ba}+i\gamma}\\
&\qquad+i\mathcal{A}^{\mu}_{ab}(\boldsymbol{k})h^{\alpha_1}_{\boldsymbol{k}aa}h^{\alpha_2}_{\boldsymbol{k}ba}\frac{f_{ab}}{\omega_2-\varepsilon_{\boldsymbol{k}ba}+i\gamma}+i\mathcal{A}^{\mu}_{cb}(\boldsymbol{k})h^{\alpha_1}_{\boldsymbol{k}ac}h^{\alpha_2}_{\boldsymbol{k}ba}\frac{f_{ab}}{\omega_2-\varepsilon_{\boldsymbol{k}ba}+i\gamma}+[(\omega_1,\alpha_1)\longleftrightarrow(\omega_2,\alpha_2)]\Bigg],
\end{aligned}
\tag{C65}
$$

where we switched $a\leftrightarrow c$ in the first term. Similarly, the summation of c is decomposed into $c=b$ part and $c\neq b$ part. Then, for $c\neq b$ part, the role of dummy variables a and b can be switched safely. Thus,

$$
\begin{aligned}
&\langle \widehat{J}^{\mu}_{\rm shift}\rangle^{(2)}(\omega)\\
&=\frac{1}{2}\sum_{abc(a\neq c,\,b\neq c)}\int\frac{d^d\boldsymbol{k}}{(2\pi)^d}\int d\omega_1 d\omega_2\left(\frac{-e^3}{\omega_1\omega_2}\right)E^{\alpha_1}(\omega_1)E^{\alpha_2}(\omega_2)\delta(\omega-\omega_1-\omega_2)\\
&\quad\times\Bigg[i\mathcal{A}^{\mu}_{ba}(\boldsymbol{k})h^{\alpha_1}_{\boldsymbol{k}ab}h^{\alpha_2}_{\boldsymbol{k}bb}\frac{f_{ab}}{\omega_1-\varepsilon_{\boldsymbol{k}ab}+i\gamma}+i\mathcal{A}^{\mu}_{ca}(\boldsymbol{k})h^{\alpha_1}_{\boldsymbol{k}ab}h^{\alpha_2}_{\boldsymbol{k}bc}\frac{f_{ab}}{\omega_1-\varepsilon_{\boldsymbol{k}ab}+i\gamma}+\partial_{k^\mu}h^{\alpha_1}_{\boldsymbol{k}ab}h^{\alpha_2}_{\boldsymbol{k}ba}\frac{f_{ab}}{\omega_2-\varepsilon_{\boldsymbol{k}ba}+i\gamma}\\
&\qquad-i\mathcal{A}^{\mu}_{aa}(\boldsymbol{k})h^{\alpha_1}_{\boldsymbol{k}ab}h^{\alpha_2}_{\boldsymbol{k}ba}\frac{f_{ab}}{\omega_2-\varepsilon_{\boldsymbol{k}ba}+i\gamma}+i\mathcal{A}^{\mu}_{ab}(\boldsymbol{k})h^{\alpha_1}_{\boldsymbol{k}aa}h^{\alpha_2}_{\boldsymbol{k}ba}\frac{f_{ab}}{\omega_2-\varepsilon_{\boldsymbol{k}ba}+i\gamma}\\
&\qquad+i\mathcal{A}^{\mu}_{bb}(\boldsymbol{k})h^{\alpha_1}_{\boldsymbol{k}ab}h^{\alpha_2}_{\boldsymbol{k}ba}\frac{f_{ab}}{\omega_2-\varepsilon_{\boldsymbol{k}ba}+i\gamma}+i\mathcal{A}^{\mu}_{cb}(\boldsymbol{k})h^{\alpha_1}_{\boldsymbol{k}ac}h^{\alpha_2}_{\boldsymbol{k}ba}\frac{f_{ab}}{\omega_2-\varepsilon_{\boldsymbol{k}ba}+i\gamma}+[(\omega_1,\alpha_1)\longleftrightarrow(\omega_2,\alpha_2)]\Bigg]\\
&=\frac{1}{2}\sum_{abc(a\neq c,\,b\neq c)}\int\frac{d^d\boldsymbol{k}}{(2\pi)^d}\int d\omega_1 d\omega_2\left(\frac{-e^3}{\omega_1\omega_2}\right)E^{\alpha_1}(\omega_1)E^{\alpha_2}(\omega_2)\delta(\omega-\omega_1-\omega_2)\\
&\quad\times\Bigg[i\mathcal{A}^{\mu}_{ba}(\boldsymbol{k})h^{\alpha_1}_{\boldsymbol{k}ab}h^{\alpha_2}_{\boldsymbol{k}bb}\frac{f_{ab}}{\omega_1-\varepsilon_{\boldsymbol{k}ab}+i\gamma}+i\mathcal{A}^{\mu}_{ca}(\boldsymbol{k})h^{\alpha_1}_{\boldsymbol{k}ab}h^{\alpha_2}_{\boldsymbol{k}bc}\frac{f_{ab}}{\omega_1-\varepsilon_{\boldsymbol{k}ab}+i\gamma}+\partial_{k^\mu}h^{\alpha_1}_{\boldsymbol{k}ab}h^{\alpha_2}_{\boldsymbol{k}ba}\frac{f_{ab}}{\omega_2-\varepsilon_{\boldsymbol{k}ba}+i\gamma}\\
&\qquad-i\mathcal{A}^{\mu}_{aa}(\boldsymbol{k})h^{\alpha_1}_{\boldsymbol{k}ab}h^{\alpha_2}_{\boldsymbol{k}ba}\frac{f_{ab}}{\omega_2-\varepsilon_{\boldsymbol{k}ba}+i\gamma}+i\mathcal{A}^{\mu}_{ab}(\boldsymbol{k})h^{\alpha_1}_{\boldsymbol{k}aa}h^{\alpha_2}_{\boldsymbol{k}ba}\frac{f_{ab}}{\omega_2-\varepsilon_{\boldsymbol{k}ba}+i\gamma}\\
&\qquad+i\mathcal{A}^{\mu}_{bb}(\boldsymbol{k})h^{\alpha_1}_{\boldsymbol{k}ab}h^{\alpha_2}_{\boldsymbol{k}ba}\frac{f_{ab}}{\omega_2-\varepsilon_{\boldsymbol{k}ba}+i\gamma}-i\mathcal{A}^{\mu}_{ca}(\boldsymbol{k})h^{\alpha_1}_{\boldsymbol{k}ab}h^{\alpha_2}_{\boldsymbol{k}bc}\frac{f_{ab}}{\omega_1-\varepsilon_{\boldsymbol{k}ab}+i\gamma}+[(\omega_1,\alpha_1)\longleftrightarrow(\omega_2,\alpha_2)]\Bigg]\\
&=\frac{1}{2}\sum_{ab}\int\frac{d^d\boldsymbol{k}}{(2\pi)^d}\int d\omega_1 d\omega_2\left(\frac{-e^3}{\omega_1\omega_2}\right)E^{\alpha_1}(\omega_1)E^{\alpha_2}(\omega_2)\delta(\omega-\omega_1-\omega_2)\\
&\quad\times\Bigg[\partial_{k^\mu}h^{\alpha_1}_{\boldsymbol{k}ab}h^{\alpha_2}_{\boldsymbol{k}ba}\frac{f_{ab}}{\omega_2-\varepsilon_{\boldsymbol{k}ba}+i\gamma}+i\mathcal{A}^{\mu}_{ba}(\boldsymbol{k})h^{\alpha_1}_{\boldsymbol{k}ab}h^{\alpha_2}_{\boldsymbol{k}bb}\frac{f_{ab}}{\omega_1-\varepsilon_{\boldsymbol{k}ab}+i\gamma}-i\mathcal{A}^{\mu}_{aa}(\boldsymbol{k})h^{\alpha_1}_{\boldsymbol{k}ab}h^{\alpha_2}_{\boldsymbol{k}ba}\frac{f_{ab}}{\omega_2-\varepsilon_{\boldsymbol{k}ba}+i\gamma}\\
&\qquad+i\mathcal{A}^{\mu}_{ab}(\boldsymbol{k})h^{\alpha_1}_{\boldsymbol{k}aa}h^{\alpha_2}_{\boldsymbol{k}ba}\frac{f_{ab}}{\omega_2-\varepsilon_{\boldsymbol{k}ba}+i\gamma}+i\mathcal{A}^{\mu}_{bb}(\boldsymbol{k})h^{\alpha_1}_{\boldsymbol{k}ab}h^{\alpha_2}_{\boldsymbol{k}ba}\frac{f_{ab}}{\omega_2-\varepsilon_{\boldsymbol{k}ba}+i\gamma}+[(\omega_1,\alpha_1)\longleftrightarrow(\omega_2,\alpha_2)]\Bigg].
\end{aligned}
\tag{C66}
$$

We write $[(\omega_1,\alpha_1)\longleftrightarrow(\omega_2,\alpha_2)]$ part explicitly:

$$
\begin{aligned}
&\langle \widehat{J}^{\mu}_{\rm shift}\rangle^{(2)}(\omega)\\
&=\frac{1}{2}\sum_{ab}\int\frac{d^d\boldsymbol{k}}{(2\pi)^d}\int d\omega_1 d\omega_2\left(\frac{-e^3}{\omega_1\omega_2}\right)E^{\alpha_1}(\omega_1)E^{\alpha_2}(\omega_2)\delta(\omega-\omega_1-\omega_2)\\
&\quad\times\Bigg[\partial_{k^\mu}h^{\alpha_1}_{\boldsymbol{k}ab}h^{\alpha_2}_{\boldsymbol{k}ba}\frac{f_{ab}}{\omega_2-\varepsilon_{\boldsymbol{k}ba}+i\gamma}+i\mathcal{A}^{\mu}_{ba}(\boldsymbol{k})h^{\alpha_1}_{\boldsymbol{k}ab}h^{\alpha_2}_{\boldsymbol{k}bb}\frac{f_{ab}}{\omega_1-\varepsilon_{\boldsymbol{k}ab}+i\gamma}-i\mathcal{A}^{\mu}_{aa}(\boldsymbol{k})h^{\alpha_1}_{\boldsymbol{k}ab}h^{\alpha_2}_{\boldsymbol{k}ba}\frac{f_{ab}}{\omega_2-\varepsilon_{\boldsymbol{k}ba}+i\gamma}\\
&\qquad+i\mathcal{A}^{\mu}_{ab}(\boldsymbol{k})h^{\alpha_1}_{\boldsymbol{k}aa}h^{\alpha_2}_{\boldsymbol{k}ba}\frac{f_{ab}}{\omega_2-\varepsilon_{\boldsymbol{k}ba}+i\gamma}+i\mathcal{A}^{\mu}_{bb}(\boldsymbol{k})h^{\alpha_1}_{\boldsymbol{k}ab}h^{\alpha_2}_{\boldsymbol{k}ba}\frac{f_{ab}}{\omega_2-\varepsilon_{\boldsymbol{k}ba}+i\gamma}\\
&\qquad+\partial_{k^\mu}h^{\alpha_2}_{\boldsymbol{k}ab}h^{\alpha_1}_{\boldsymbol{k}ba}\frac{f_{ab}}{\omega_1-\varepsilon_{\boldsymbol{k}ba}+i\gamma}+i\mathcal{A}^{\mu}_{ba}(\boldsymbol{k})h^{\alpha_2}_{\boldsymbol{k}ab}h^{\alpha_1}_{\boldsymbol{k}bb}\frac{f_{ab}}{\omega_2-\varepsilon_{\boldsymbol{k}ab}+i\gamma}-i\mathcal{A}^{\mu}_{aa}(\boldsymbol{k})h^{\alpha_2}_{\boldsymbol{k}ab}h^{\alpha_1}_{\boldsymbol{k}ba}\frac{f_{ab}}{\omega_1-\varepsilon_{\boldsymbol{k}ba}+i\gamma}\\
&\qquad+i\mathcal{A}^{\mu}_{ab}(\boldsymbol{k})h^{\alpha_2}_{\boldsymbol{k}aa}h^{\alpha_1}_{\boldsymbol{k}ba}\frac{f_{ab}}{\omega_1-\varepsilon_{\boldsymbol{k}ba}+i\gamma}+i\mathcal{A}^{\mu}_{bb}(\boldsymbol{k})h^{\alpha_2}_{\boldsymbol{k}ab}h^{\alpha_1}_{\boldsymbol{k}ba}\frac{f_{ab}}{\omega_1-\varepsilon_{\boldsymbol{k}ba}+i\gamma}\Bigg]\\
&=\frac{1}{2}\sum_{ab}\int\frac{d^d\boldsymbol{k}}{(2\pi)^d}\int d\omega_1 d\omega_2\left(\frac{-e^3}{\omega_1\omega_2}\right)E^{\alpha_1}(\omega_1)E^{\alpha_2}(\omega_2)\delta(\omega-\omega_1-\omega_2)\\
&\quad\times\Bigg[\partial_{k^\mu}h^{\alpha_1}_{\boldsymbol{k}ab}h^{\alpha_2}_{\boldsymbol{k}ba}\frac{f_{ab}}{\omega_2-\varepsilon_{\boldsymbol{k}ba}+i\gamma}+i\mathcal{A}^{\mu}_{ba}(\boldsymbol{k})h^{\alpha_1}_{\boldsymbol{k}ab}h^{\alpha_2}_{\boldsymbol{k}bb}\frac{f_{ab}}{\omega_1-\varepsilon_{\boldsymbol{k}ab}+i\gamma}-i\mathcal{A}^{\mu}_{aa}(\boldsymbol{k})h^{\alpha_1}_{\boldsymbol{k}ab}h^{\alpha_2}_{\boldsymbol{k}ba}\frac{f_{ab}}{\omega_2-\varepsilon_{\boldsymbol{k}ba}+i\gamma}\\
&\qquad+i\mathcal{A}^{\mu}_{ab}(\boldsymbol{k})h^{\alpha_1}_{\boldsymbol{k}aa}h^{\alpha_2}_{\boldsymbol{k}ba}\frac{f_{ab}}{\omega_2-\varepsilon_{\boldsymbol{k}ba}+i\gamma}+i\mathcal{A}^{\mu}_{bb}(\boldsymbol{k})h^{\alpha_1}_{\boldsymbol{k}ab}h^{\alpha_2}_{\boldsymbol{k}ba}\frac{f_{ab}}{\omega_2-\varepsilon_{\boldsymbol{k}ba}+i\gamma}\\
&\qquad+h^{\alpha_1}_{\boldsymbol{k}ba}\partial_{k^\mu}h^{\alpha_2}_{\boldsymbol{k}ab}\frac{f_{ab}}{\omega_1-\varepsilon_{\boldsymbol{k}ba}+i\gamma}-i\mathcal{A}^{\mu}_{ab}(\boldsymbol{k})h^{\alpha_1}_{\boldsymbol{k}aa}h^{\alpha_2}_{\boldsymbol{k}ba}\frac{f_{ab}}{\omega_2-\varepsilon_{\boldsymbol{k}ba}+i\gamma}-i\mathcal{A}^{\mu}_{aa}(\boldsymbol{k})h^{\alpha_1}_{\boldsymbol{k}ba}h^{\alpha_2}_{\boldsymbol{k}ab}\frac{f_{ab}}{\omega_1-\varepsilon_{\boldsymbol{k}ba}+i\gamma}\\
&\qquad-i\mathcal{A}^{\mu}_{ba}(\boldsymbol{k})h^{\alpha_1}_{\boldsymbol{k}ab}h^{\alpha_2}_{\boldsymbol{k}bb}\frac{f_{ab}}{\omega_1-\varepsilon_{\boldsymbol{k}ab}+i\gamma}+i\mathcal{A}^{\mu}_{bb}(\boldsymbol{k})h^{\alpha_1}_{\boldsymbol{k}ba}h^{\alpha_2}_{\boldsymbol{k}ab}\frac{f_{ab}}{\omega_1-\varepsilon_{\boldsymbol{k}ba}+i\gamma}\Bigg]\\
&=\frac{1}{2}\sum_{ab}\int\frac{d^d\boldsymbol{k}}{(2\pi)^d}\int d\omega_1 d\omega_2\left(\frac{-e^3}{\omega_1\omega_2}\right)E^{\alpha_1}(\omega_1)E^{\alpha_2}(\omega_2)\delta(\omega-\omega_1-\omega_2)\\
&\quad\times\left[\left(\partial_{k^\mu}h^{\alpha_1}_{\boldsymbol{k}ab}-i\mathcal{A}^{\mu}_{aa}(\boldsymbol{k})h^{\alpha_1}_{\boldsymbol{k}ab}+i\mathcal{A}^{\mu}_{bb}(\boldsymbol{k})h^{\alpha_1}_{\boldsymbol{k}ab}\right)h^{\alpha_2}_{\boldsymbol{k}ba}\frac{f_{ab}}{\omega_2-\varepsilon_{\boldsymbol{k}ba}+i\gamma}+[(\omega_1,\alpha_1)\longleftrightarrow(\omega_2,\alpha_2)]\right]
\end{aligned}
\tag{C67}
$$

There remains only $a\neq b$ part since it is proportional to f_{ab}. Thus (C62) is simplified to $h^{\mu}_{\boldsymbol{k}ab}=i\varepsilon_{\boldsymbol{k}ab}\mathcal{A}^{\mu}_{ab}(\boldsymbol{k})$. Using the following shorthands:

$$
r^{\mu}_{\boldsymbol{k}ab}\equiv i\varepsilon_{\boldsymbol{k}ab}\mathcal{A}^{\mu}_{ab}(\boldsymbol{k}),\quad r^{\mu\alpha}_{\boldsymbol{k}ab}\equiv\left[\partial_{k_\mu}r^{\alpha}_{\boldsymbol{k}ab}-i\left(\mathcal{A}^{\mu}_{aa}(\boldsymbol{k})-\mathcal{A}^{\mu}_{bb}(\boldsymbol{k})\right)r^{\alpha}_{\boldsymbol{k}ab}\right],
\tag{C68}
$$

We obtain the final form of the shift current:

$$
\begin{aligned}
\langle \widehat{J}^{\mu}_{\rm shift}\rangle^{(2)}(\omega)&=\frac{1}{2}\sum_{ab}\int\frac{d^d\boldsymbol{k}}{(2\pi)^d}\int d\omega_1 d\omega_2\left(\frac{-e^3}{\omega_1\omega_2}\right)E^{\alpha_1}(\omega_1)E^{\alpha_2}(\omega_2)\delta(\omega-\omega_1-\omega_2)\\
&\quad\times\left[r^{\mu\alpha_1}_{\boldsymbol{k}ab}r^{\alpha_2}_{\boldsymbol{k}ba}\frac{f_{ab}}{\omega_2-\varepsilon_{\boldsymbol{k}ba}+i\gamma}+[(\omega_1,\alpha_1)\longleftrightarrow(\omega_2,\alpha_2)]\right].
\end{aligned}
\tag{C69}
$$

Appendix D: Derivation of optical response using real time formalism

In this appendix, we derive the optical response of the electronic system using the real-time formalism. Assume that the state is initialized as thermal equilibrium without perturbation, ρ_0, at time $t=-\infty$, the expectation value of a general operator $O(t)$ is given by

$$\langle O(t)\rangle = \frac{\mathrm{Tr}\left[\rho_0 U^\dagger(t,-\infty)O_I(t)U(t,-\infty)\right]}{\mathrm{Tr}[\rho_0]} \tag{D1}$$
$$= \frac{\mathrm{Tr}\left[\rho_0 U(-\infty,\infty)U(\infty,t)O_I(t)U(t,-\infty)\right]}{\mathrm{Tr}[\rho_0]} \tag{D2}$$
$$= \frac{\mathrm{Tr}\left[\rho_0 \mathcal{T}e^{-i\int_{\mathcal{C}}V_I(t')dt'}O_I(t)\right]}{\mathrm{Tr}[\rho_0]} \tag{D3}$$

where path $\mathcal{C}$ is from $-\infty\to\infty\to-\infty$ and time evolution operator in interaction picture U is given by

$$U(t_1,t_2)=\exp\left(-i\int_{t_1}^{t_2}V_I(t')dt'\right) \tag{D4}$$

with $V_I(t)\equiv e^{iH_0t}V(t)e^{-iH_0t}$. In the following, we use notation $\langle A\rangle_0\equiv \mathrm{Tr}[\rho_0 A]/\mathrm{Tr}[\rho_0]$ for any operator A.

In the following, we set

$$O=v^\mu\equiv -i[r^\mu,H]=-i[r^\mu,H_0+V_E] \tag{D5}$$

corresponding to the current operator in the presence of electromagnetic fields. Here, for simplicity, we set $e=1,\hbar=1$ and omit parameter k and its integration for simplicity. Note that Hamiltonian H is given by Eq. (B22) and V_E is defined by Eq. (B25).

1. Linear order

Here, we assume field $\boldsymbol{E}(t)=\boldsymbol{E}e^{-i\omega t+\gamma t}$, where γ is small positive constant, and the factor $e^{\gamma t}$ added for the convergence at $t\to-\infty$. Note that velocity operator given by Eq. (D5) depends on electric field as well. Expanding the above equation, we have

$$\begin{aligned}\langle v^\mu(t)\rangle^{(1)} &= \langle v_I^\mu(t)\rangle_0 - i\langle v_I^\mu(t)\int_{-\infty}^{t}dt_1 V_I(t_1)\rangle_0 - i\langle\int_{t}^{-\infty}dt_1 V_I(t_1)v_I^\mu(t)\rangle_0\\ &= e^{-i\omega t}\frac{iE^\alpha}{\omega}f_a h^{\mu\alpha}_{aa} - \left(ie^{-i\omega t}\frac{iE^\alpha}{\omega}f_a\int_{-\infty}^{t}dt_1 e^{+i\omega(t-t_1)}h^\mu_{ab}h^\alpha_{ba}e^{i\varepsilon_a(t-t_1)}e^{-i\varepsilon_b(t-t_1)}e^{\gamma t_1}-(\mu\leftrightarrow\alpha)\right)\\ &= e^{-i\omega t}\frac{iE^\alpha}{\omega}\left(f_a h^{\mu\alpha}_{aa}+h^\mu_{ab}h^\alpha_{ba}\left[\frac{f_{ab}}{(\omega-\varepsilon_{ba})+i\gamma}\right]\right)\end{aligned} \tag{D6}$$

where

$$f_a\equiv\langle\psi_a|\rho_0|\psi_a\rangle/\mathrm{Tr}[\rho_0], \tag{D7}$$

where $|\psi_a\rangle$ represents an eigenstate a. We insert the complete set between operators to obtain the second equation of Eq. (D6).

2. Second order

Assume field $\boldsymbol{E}(t) = \boldsymbol{E}_1 e^{-i\omega_1 t+\gamma t} + \boldsymbol{E}_2 e^{-i\omega_2 t+\gamma t}$. Expand the term including two fields and insert complete sets between every operators, similarly as in the case of linear order, we obtain

$$\begin{aligned}\langle v^\mu(t)\rangle^{(2)} =& \langle v_I^\mu(t)\rangle_0 - i\langle v_I^\mu(t)\int_{-\infty}^t dt_1 V_I(t_1)\rangle_0 - i\langle\int_t^{-\infty} dt_1 V_I(t_1) v_I^\mu(t)\rangle_0 \\ & - \langle v^\mu(t)\int_{-\infty}^t dt_2 \int_{-\infty}^{t_2} dt_1 V_I(t_2)V_I(t_1)\rangle_0 - \langle\int_t^{-\infty} dt_2 V_I(t_2) v^\mu(t)\int_{-\infty}^t dt_1 V_I(t_1)\rangle_0 \\ & - \langle\int_{t_2}^{-\infty} dt_1 \int_t^{-\infty} dt_2 V_I(t_1)V_I(t_2) v^\mu(t)\rangle_0 \end{aligned} \tag{D8}$$

For the first, second and third term in rhs of Eq. (D8), we obtain

$$\begin{aligned}(\text{first, second and third term}) =& \frac{E_1^\alpha E_2^\beta}{-\omega_1\omega_2} e^{-i\omega_1 t} e^{-i\omega_2 t}\left(h_{ab}^{\mu\alpha} h_{ba}^\beta \left[\frac{f_{ab}}{(\omega_2-\varepsilon_{ba})+i\gamma}\right]\right. \\ & \left. + h_{ab}^\mu h_{ba}^{\alpha\beta}\left[\frac{f_{ab}}{(\omega_1+\omega_2-\varepsilon_{ba})+i\gamma}\right] + h_{aa}^{\mu\alpha\beta} f_a\right) + (\alpha,\omega_1 \leftrightarrow \beta,\omega_2). \end{aligned} \tag{D9}$$

For the fourth term in rhs of Eq. (D8), we get

$$\begin{aligned}(\text{fourth term}) =& - h_{ab}^\mu h_{bc}^\alpha h_{ca}^\beta \frac{E_1^\alpha E_2^\beta}{-\omega_1\omega_2} e^{-i\omega_1 t} e^{-i\omega_2 t} f_a \\ & \times \int_{-\infty}^t dt_2 \int_{-\infty}^{t_2} dt_1 e^{-i\omega_1(t_2-t)} e^{-i\omega_2(t_1-t)} e^{\gamma(t_1+t_2)} e^{-i\varepsilon_b(t-t_2)} e^{-i\varepsilon_c(t_2-t_1)} e^{-i\varepsilon_a(t_1-t)} \\ & + (\alpha, 1 \leftrightarrow \beta, 2) \\ =& - \frac{h_{ab}^\mu h_{bc}^\alpha h_{ca}^\beta E_1^\alpha E_2^\beta e^{-i\omega_1 t} e^{-i\omega_2 t} f_a}{[i(-\omega_2+\varepsilon_c-\varepsilon_a)+\gamma][i(-\omega_1-\omega_2-\varepsilon_a+\varepsilon_b)+\gamma]} + (\alpha,\omega_1 \leftrightarrow \beta,\omega_2). \end{aligned} \tag{D10}$$

Performing a similar calculation for other terms, we arrive at the following result.

$$\begin{aligned}\langle v^\mu(t)\rangle^{(2)} =& \frac{E_1^\alpha E_2^\beta}{-\omega_1\omega_2} e^{-i\omega_1 t} e^{-i\omega_2 t}\left(h_{ab}^{\mu\alpha} h_{ba}^\beta \left[\frac{f_{ab}}{(\omega_2-\varepsilon_{ba})+i\gamma}\right] + h_{ab}^\mu h_{ba}^{\alpha\beta}\left[\frac{f_{ab}}{(\omega_1+\omega_2-\varepsilon_{ba})+i\gamma}\right] + h_{aa}^{\mu\alpha\beta} f_a\right) \\ & + h_{ab}^\mu h_{bc}^\alpha h_{ca}^\beta \frac{E_1^\alpha E_2^\beta}{-\omega_1\omega_2} e^{-i\omega_1 t} e^{-i\omega_2 t} \times \left(\frac{f_a}{[(\omega_2-\varepsilon_{ca})+i\gamma][(\omega-\varepsilon_{ba})+i2\gamma]} \right. \\ & \left. - \frac{f_c}{[(\omega_2-\varepsilon_{ca})+i\gamma][\omega_1-\varepsilon_{bc})+i\gamma]} + \frac{f_b}{[(\omega_1-\varepsilon_{bc})+i\gamma][(\omega-\varepsilon_{ba})+i2\gamma]}\right) \\ & + (\alpha,\omega_1 \leftrightarrow \beta,\omega_2) \\ =& \frac{E_1^\alpha E_2^\beta}{-\omega_1\omega_2} e^{-i\omega_1 t} e^{-i\omega_2 t}\left(h_{ab}^{\mu\alpha} h_{ba}^\beta \left[\frac{f_{ab}}{(\omega_2-\varepsilon_{ba})+i\gamma}\right] + h_{ab}^\mu h_{ba}^{\alpha\beta}\left[\frac{f_{ab}}{(\omega_1+\omega_2-\varepsilon_{ba})+i\gamma}\right] + h_{aa}^{\mu\alpha\beta} f_a\right. \\ & \left. + h_{ab}^\mu h_{bc}^\alpha h_{ca}^\beta \left[\frac{f_{ac}(\omega_1-\varepsilon_{bc}+i\gamma)+f_{bc}(\omega_2-\varepsilon_{ca}+i\gamma)}{(\omega_1-\varepsilon_{bc}+i\gamma)(\omega_2-\varepsilon_{ca}+i\gamma)(\omega-\varepsilon_{ba}+i2\gamma)}\right]\right) \\ & + (\alpha,\omega_1 \leftrightarrow \beta,\omega_2) \end{aligned} \tag{D11}$$

The results coincides with those derived using coherent path integral formalism presented in Appendix C.

Appendix E: Rice-mele model

The Rice-Mele model is the simplest model capturing important features of conductivity with two input fields. It consists of two types (A, B) of ions as a unit cell aligned repeatedly in a 1-dimensional line, and the electron state is described by a tight-binding model. The potential for an electron to be localized at ion A or B is V_A and V_B, respectively, while the hopping energy is t. In this model, the spatial inversion symmetry is broken when $V_A \neq V_B$, and the displacement between Bloch states causes the shift current. The electron Hamiltonian matrix is given by:

$$H(k) = \boldsymbol{d}(k) \cdot \boldsymbol{\sigma}, \tag{E1}$$

where $\boldsymbol{\sigma} = \{\sigma_x, \sigma_y, \sigma_z\}$ with $\sigma_{x,y,z}$ denoting Pauli matrices, $d_x = t(1 + \cos ka), d_y = -t \sin ka$, and $d_z = (V_A - V_B)/2$. The energy level and the corresponding Bloch state are

$$\varepsilon_\pm = \pm|\boldsymbol{d}|, \tag{E2}$$

$$|u_\pm\rangle = \begin{pmatrix} \frac{d_z \pm |\boldsymbol{d}|}{d_x + i d_y} \\ 1 \end{pmatrix}. \tag{E3}$$

As a concrete example, we show the band structure in FIG. 4. We have used the parameter set: $t = 100$ meV and $V_A = 30$ meV, $V_B = 0$ meV, referring to the scale of typical electronic systems and topological insulators (Ref [47, 65]). The band gap and the covering energy scale are determined by $|V_A - V_B|$ and t, respectively.

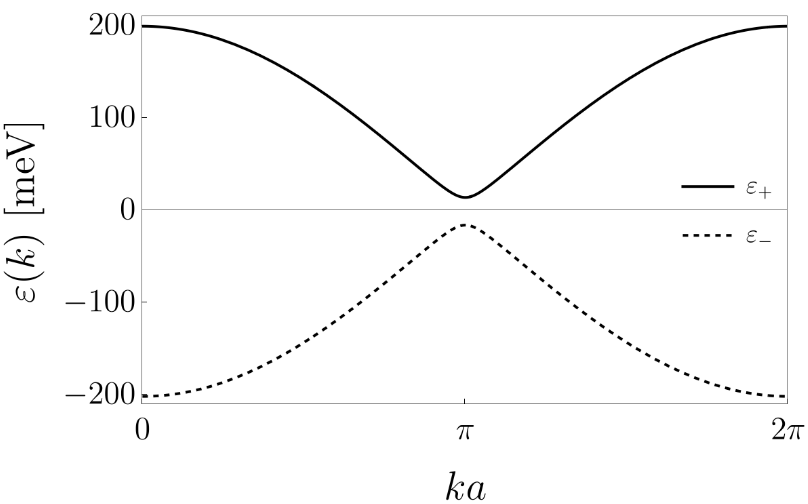

FIG. 4. Band structure of Rice-Mele model. The potential of each site is $V_A = 30$ meV, $V_B = 0$ meV, while the hopping energy is $t = 100$ meV. The spatial inversion symmetry is broken due to $V_A \neq V_B$, allowing the spatial shift of states.